
CONTINUOUS TIME LOCALLY STATIONARY WAVELET PROCESSES

Henry Antonio Palasciano

Department of Mathematics
Imperial College London
SW7 2AZ, London, UK

henry.palasciano17@imperial.ac.uk

Marina I. Knight

Department of Mathematics
University of York
YO10 5DD, York, UK

marina.knight@york.ac.uk

Guy P. Nason

Department of Mathematics
Imperial College London
SW7 2AZ, London, UK

g.nason@imperial.ac.uk

October 20, 2023

ABSTRACT

This article introduces the class of continuous time locally stationary wavelet processes. Continuous time models enable us to properly provide scale-based time series models for irregularly-spaced observations for the first time. We derive results for both the theoretical setting, where we assume access to the entire process sample path, and a more practical one, which develops methods for estimating the quantities of interest from sampled time series. The latter estimates are accurately computable in reasonable time by solving the relevant linear integral equation using the iterative thresholding method due to Daubechies, Defrise and De Mol. We exemplify our new methods by computing spectral and autocovariance estimates on irregularly-spaced heart-rate data obtained from a recent sleep-state study.

Keywords Continuous time models, Irregular spacing, Local autocovariance, Non-stationary time series, Wavelets, Wavelet spectrum

1 Introduction

It is often customary to assume that a time series is (second-order) stationary, since, in this case, plenty of theoretically sound and well-tested methods are readily available for its analysis, see, e.g., [1] or [2]. However, in practice, many time series are unlikely to be stationary. For example, many financial time series are often non-stationary [3, 4, 5, 6]. It is well known that a stationary stochastic process $X(t)$, $t \in \mathbb{R}$, has a spectral representation of the form

$$X(t) = \int_{-\infty}^{\infty} \exp(i\omega t) dZ(\omega), \quad (1)$$

where $Z(\omega)$ is a square-integrable orthogonal increment process satisfying $\mathbb{E} [|dZ(\omega)|^2] = dS(\omega)$ and $S(\omega)$ is the integrated spectrum of $X(t)$. The autocovariance function of $X(t)$, $c(\tau)$, has a similar representation in the frequency domain,

$$c(\tau) = \int_{-\infty}^{\infty} \exp(i\omega\tau) dS(\omega), \quad (2)$$

see, e.g., [7]. To extend these quantities to the non-stationary case, [7] suggested introducing a time-varying amplitude function $A(t, \omega)$ into (1) giving

$$X(t) = \int_{-\infty}^{\infty} A(t, \omega) \exp(i\omega t) dZ(\omega). \quad (3)$$

Models such as (3) form the basis for locally stationary time series, later developed by [8] in discrete time.

[9] introduced the locally stationary *wavelet* (LSW) processes, which replaced the set of functions $\{\exp(i\omega t)\}$ with a set of discrete non-decimated wavelets. As with locally stationary Fourier processes [8], the process local

stationarity is enforced via constraints on their amplitude functions. From LSW processes, one can then obtain a time-scale decomposition of the spectral density function, known as the evolutionary wavelet spectrum, and a wavelet representation of the local autocovariance similar to (2).

However, discrete time LSW processes are constructed under the assumption that the time series data is obtained at a constant rate, which is not always appropriate as, in practice, observations can either be missing or be irregularly-spaced. Attempts to provide a suitable alternative for irregularly-spaced data were made in [10] and [11] via the use of second-generation wavelets. Unfortunately, spectral estimates obtained through these attempts only somewhat resemble those in [9] and can be computationally expensive. This article proposes the use of continuous time locally stationary wavelet processes instead, which are natural counterparts to the discrete time versions developed in [9]. To our knowledge, our new methods are the only ones that can accurately estimate wavelet spectral properties of an irregularly-sampled process within a reasonable computational time frame.

Aside from the practical advantages that a continuous time model provides, our results are also interesting from a more theoretical perspective. In fact, many discrete time models and methods also possess a continuous time counterpart, see [12], [13], [14] and [15] for example. Recently, [16] adapted locally stationary Fourier processes from the discrete (see [8] or [17]) to the continuous time setting. Since, so far, the theory of LSW processes [9] exists in discrete time only, our objective is to introduce parallel continuous time models, study their theoretical properties and develop a practical means for their estimation and analysis. In doing so, we obtain a representation of the evolutionary wavelet spectrum across a *continuous* range of scales, providing a complete decomposition of the underlying frequencies of the process.

Section 2 reviews relevant background material on locally stationary processes in discrete time, Lévy processes and bases, and useful regularisation methods. Section 3 defines our locally stationary wavelet processes, its associated evolutionary wavelet spectrum and local autocovariance, and related concepts all in continuous time. Section 4 demonstrates how these continuous time models can be fitted to irregularly spaced time series. Finally, Section 5 shows the effectiveness of our methods by computing an estimate of the continuous time evolutionary wavelet spectrum to irregularly-spaced heart rate measurements of a sleeping individual and compares this estimate to the corresponding sleep stage time series. Such comparisons can be used to predict expensive and hard to collect sleep stage series from heart rate series that are cheaper and easier to collect, particularly in the home environment.

2 Background

We next briefly review some of the necessary background material beginning with locally stationary wavelet processes in discrete time, followed by Lévy bases and conclude with some useful regularisation methods. A more comprehensive review can be found in Supplementary Materials Section A.

(Discrete) locally stationary wavelet (LSW) processes [9, 18] are time series models that have found applications in various domains, including finance [6], economics [19] alias detection [20, 21], gravitational-wave detection [22] and energy [23, 24], to name but a few. They are defined as a sequence of stochastic processes indexed by time and have the following representation in the mean square sense:

$$X_{t,T} = \sum_{j=1}^{\infty} \sum_{k=-\infty}^{\infty} w_{j,k;T} \psi_{j,k-t} \xi_{j,k}, \quad (4)$$

where $\{w_{j,k;T}\}_{j \in \mathbb{N}, k \in \mathbb{Z}}$ is a set of amplitudes, $\{\psi_{j,k-t}\}_{j \in \mathbb{N}, k \in \mathbb{Z}}$ are discrete wavelets and $\{\xi_{j,k}\}_{j \in \mathbb{N}, k \in \mathbb{Z}}$ is a set of random variables with zero mean and unit variance. Conditions are also imposed on the amplitude functions to prevent them from varying too quickly, thus preserving the local stationarity of the process. More importantly, one assumes that, as $T \rightarrow \infty$, $w_{j,k;T}$ converges to $W_j(k/T)$, a rescaled time Lipschitz continuous amplitude function defined on $z = k/T \in (0, 1)$, which is known as rescaled time (introduced by [8]) and which is commonly employed when working with locally stationary processes. One can then also define the evolutionary wavelet spectrum of the LSW process by

$$S_j(z) = |W_j(z)|^2 \quad (5)$$

and the autocorrelation wavelets and local autocovariance by

$$\Psi_j(\tau) = \sum_k \psi_{j,k} \psi_{j,k-\tau}, \quad \text{and} \quad c(z, \tau) = \sum_{j=1}^{\infty} S_j(z) \Psi_j(\tau), \quad (6)$$

respectively, where $j \in \mathbb{N}$ and $\tau \in \mathbb{Z}$. To estimate the spectrum, one can use the non-decimated discrete wavelet transform to compute the raw wavelet periodogram and then correct this using an inner product operator. For more details see [9].

Lévy processes and bases play a crucial role in the definition of locally stationary wavelet processes in continuous time. Our discussion draws heavily from [25, 26, 27, 28, 29]. In the following, take $(\Omega, \mathcal{F}, \mathbb{P})$ to be the underlying probability space, $(S, \mathcal{B}(S))$ to be a Borel space and denote the bounded Borel sets of $\mathcal{B}(S)$ by $\mathcal{B}_b(S)$. A real valued Lévy basis on S is a collection $\{L(A) : A \in \mathcal{B}_b(S)\}$ of random variables satisfying the following properties:

(a) If A and B are disjoint subsets in $\mathcal{B}_b(S)$, then

$$L(A \cup B) = L(A) + L(B), \quad \text{almost surely.} \quad (7)$$

(b) If A and B are disjoint subsets in $\mathcal{B}_b(S)$, then $L(A)$ and $L(B)$ are independent,

(c) The law of $L(A)$ is infinitely divisible for all $A \in \mathcal{B}_b(S)$.

Since the law of $L(A)$ for all $A \in \mathcal{B}_b(S)$ it is infinitely divisible, it has a Lévy-Khintchine representation. We restrict our attention to homogeneous Lévy bases, which is synonymous with the concept of stationarity, as defined by [25]. A homogeneous Gaussian Lévy basis G , for example, is defined as $G(A) \sim \mathcal{N}\{\mu \text{Leb}(A), \sigma^2 \text{Leb}(A)\}$ for all $A \in \mathcal{B}(\mathbb{R}^n)$, for some $\mu \in \mathbb{R}$ and $\sigma \in \mathbb{R}^+$ and where Leb denotes the Lebesgue measure, and is equivalent to the concept of white noise as defined in [28]. Furthermore, if L is a homogeneous Lévy basis on $(\mathbb{R}, \mathcal{B}(\mathbb{R}))$, then the process $(L_t)_{t \geq 0}$ with $L_t = L([0, t])$ is a Lévy process and, conversely, given a Lévy process $(L_t)_{t \geq 0}$, we can obtain a Lévy basis L by setting $L((s, t]) = L_t - L_s$.

Linear integral equations, the methods to solve them and regularisation methods for solving linear inverse problems are used here for computing evolutionary wavelet spectral estimates. We summarise key ideas from [30, 31, 32, 33]. Linear integral operators are mappings from $L^2(S)$ to $L^2(S)$, where $S \subset \mathbb{R}^n$, of the form

$$(Th)(x) = \int_S K(x, y)h(y) dy, \quad x \in S, \quad (8)$$

where $K : S \times S \mapsto \mathbb{R}$ is a continuous kernel. For our work, Mercer's ([30]) theorem is key, as we work with continuous symmetric non-negative definite kernels. Hence, the kernel K can be expanded in terms of its eigenvalues λ_n and eigenfunctions φ_n of T as

$$K(x, y) = \sum_{n=1}^{\infty} \lambda_n \varphi_n(x) \varphi_n(y), \quad (9)$$

where the convergence is absolute and uniform. Given f and K , Mercer's theorem permits us to obtain a solution h the linear integral equation $Th = f$ in terms of the eigendecomposition of K . In the presence of noise, regularisation methods such as the spectral cut-off can be employed as well.

Alternatively, (8) can be reformulated as an optimisation problem to minimise $\Delta h = \|Th - f\|^2$. In the presence of noise, several useful regularisation techniques, such as Tikhonov regularisation, are readily available. Here, we find the iterative thresholding algorithm introduced by [32] particularly useful. We minimise

$$\Phi_{\mathbf{w}, p}(h) = \|Th - f\|^2 + \sum_{\gamma \in \Gamma} w_\gamma |\langle h, e_\gamma \rangle|^p, \quad (10)$$

where $\{e_\gamma\}_{\gamma \in \Gamma}$ is an orthogonal basis of the Hilbert space H , $\mathbf{w} = \{w_\gamma\}_{\gamma \in \Gamma}$ is a vector of weights and $1 \leq p \leq 2$. In particular, we will be interested in the case where $w_\gamma = \mu > 0$ for all $\gamma \in \Gamma$ and $p = 1$. The solution can be obtained via an iterative scheme given by

$$h^n = \mathbf{S}_{\mu, 1} \{h^{n-1} + T^\dagger(f - Th^{n-1})\}, \quad (11)$$

where

$$\mathbf{S}_{\mu, 1}(h) = \sum_{\gamma} S_{\mu, 1}(\langle h, e_\gamma \rangle) e_\gamma \quad (12)$$

and

$$S_{\mu, 1}(x) = \begin{cases} x - \frac{\mu}{2}, & \text{if } x \geq \frac{\mu}{2}, \\ 0, & \text{if } |x| < \frac{\mu}{2}, \\ x + \frac{\mu}{2}, & \text{if } x \leq -\frac{\mu}{2}. \end{cases} \quad (13)$$

[32] also discuss an extension of the method where one penalises positive and negative coefficients differently, by replacing μ by μ_1 and μ_2 , which we later find particularly useful.

3 Locally Stationary Wavelet Processes in Continuous Time: Theory

Our continuous time locally stationary wavelet processes rely on continuous time wavelets $\psi \in L^2(\mathbb{R})$ for which we assume that

$$\int_{-\infty}^{\infty} \psi(x) dx = 0 \quad \text{and} \quad \|\psi\|^2 = \int_{-\infty}^{\infty} |\psi(x)|^2 dx = 1. \quad (14)$$

From $\psi \in L^2(\mathbb{R})$ an entire family of wavelets $\{\psi_{u,v}(x), u \in \mathbb{R}^+, v \in \mathbb{R}\}$ can be generated via the transformation

$$\psi_{u,v}(x) = \psi(u, x - v) = u^{-1/2} \psi\{(x - v)/u\}, \quad (15)$$

for all $u \in \mathbb{R}^+$ and $v \in \mathbb{R}$, preserving the properties in (14). For more information on the continuous wavelet transform, see [34].

As we work in continuous time, we (temporarily) assume knowledge of the entire sample path or law of the process. Consequently, unlike the discrete case, it is irrelevant to define a sequence of stochastic processes corresponding to increasing amounts of data becoming available. Hence, we define a continuous-time locally stationary wavelet process as follows.

Definition 1. (Continuous Time Locally Stationary Wavelet Process). A continuous time locally stationary wavelet process, $\{X(t)\}_{t \in \mathbb{R}}$ is defined by

$$X(t) = \int_0^{\infty} \int_{-\infty}^{\infty} W(u, v) \psi(u, t - v) L(du, dv), \quad (16)$$

where L is a homogeneous square-integrable Lévy basis with $\mathbb{E}[L(A)] = 0$ and $\mathbb{E}[L(A)^2] = \text{Leb}(A)$ for all $A \in \mathcal{B}_b(\mathbb{R}^+ \times \mathbb{R})$, $\{\psi_{u,v}(x), u \in \mathbb{R}^+, v \in \mathbb{R}\}$ is a continuous wavelet family as defined above and $W \in L^2(\mathbb{R}^+, \mathbb{R})$ is an amplitude function. Further, the following conditions on W hold:

- (a) for each fixed $u \in \mathbb{R}^+$, $W(u, \cdot)$ is a Lipschitz continuous function with Lipschitz constant function $K(u)$, which is uniformly bounded $\int_0^{\infty} uK(u)du < \infty$;
- (b) for each fixed $v \in \mathbb{R}$, $W(\cdot, v)$ satisfies $\int_0^{\infty} |W(u, v)|^2 du < \infty$.

The requirement that the Lévy basis is homogeneous is essential, as this implies that the basis is stationary and vice-versa (see Supplementary Materials Section A or [25]). This ensures that any process non-stationarity is determined entirely by the deterministic amplitude functions W . Note also that, setting $\mathbb{E}[L(A)^2] = \text{Leb}(A)$ instead of $\mathbb{E}[L(A)^2] = \sigma^2 \text{Leb}(A)$ for some $\sigma > 0$ is in no way restrictive as in our model the variance term σ^2 is absorbed directly into W .

Model Interpretation: Locally stationary processes are stochastic processes with time-varying statistical properties. Imposing the Lipschitz continuity assumptions on the amplitude function W ensures that there are no rapid variations in those statistical properties of the process. One could also impose conditions on the amplitude function W itself in order to reduce the speed at which it can vary as the scales become coarser. However, this is not necessary: in the above model, one expects the amplitude function to take large values at scale u when the oscillatory frequency of the process matches that of the wavelet or, in other words, when the correlation between $X(t)$ and $X(t \pm \tau)$ is strong for some $\tau \in \mathbb{R}$ which matches the wavelength structure of the wavelet. Due to the wavelet property just mentioned, this also ensures that the speed at which W can vary decreases as the scales become wider. Some of these ideas were discussed earlier in [9] for the discrete time version.

Remark 1. The amplitude $W(u, t)$ is defined for all $t \in \mathbb{R}$ as opposed to its discrete counterpart, which is only defined on $(0, 1)$. Later, in Section 4, when adapting this definition for practical applications, we will again return to the concept of rescaled time.

We now give an example of a continuous time locally stationary Haar wavelet process.

Definition 2. (Haar Wavelet). Let $u \in \mathbb{R}^+$, $x \in \mathbb{R}$ be the scale and location respectively. The Haar wavelet is defined by

$$\psi(u, x) = u^{-1/2} \left\{ \mathbb{1}_{[0, \frac{u}{2}]}(x) - \mathbb{1}_{[\frac{u}{2}, u]}(x) \right\}. \quad (17)$$

where $\mathbb{1}$ is the usual indicator function.

Haar wavelets provide the basic building blocks for constructing the Haar moving average processes:

Example 1 A Haar Moving Average MA(α) Process is a continuous time locally stationary wavelet process $X(t)$ with $W(u, v) = 1$ for all scales $u \in [\alpha - \eta, \alpha + \eta] \subset \mathbb{R}^+$, for some $\alpha, \eta \in \mathbb{R}^+$, and $v \in \mathbb{R}$, with Haar wavelet family

$\{\psi_{u,v}\}$, with Lévy basis $L(du, dv) = \delta_\alpha(du)G(dv)$, where $\delta_\alpha(x)$ is the Dirac delta function centred at α and $G(A)$, for $A \subset \mathbb{R}$, is a homogeneous Gaussian Lévy basis on $\mathcal{B}_b(\mathbb{R})$ and can be written as

$$X(t) = \int_0^\infty \int_{-\infty}^\infty \psi(u, t-v) \delta_\alpha(u) G(dv) = (B_t - B_{t-\alpha/2}) - (B_{t-\alpha/2} - B_{t-\alpha}), \quad (18)$$

where B_t is a standard Brownian motion. Haar moving average processes are essentially the difference of two consecutive Brownian increments, each of width $\alpha/2$. See [9] for the discrete time analogue, e.g. the Haar MA(1) and MA(2) processes are

$$X_t^1 = 2^{-1/2}(\varepsilon_t - \varepsilon_{t-1}) \quad \text{and} \quad X_t^2 = 2^{-1}(\varepsilon_t + \varepsilon_{t-1} - \varepsilon_{t-2} - \varepsilon_{t-3}), \quad (19)$$

respectively, where $\{\varepsilon_t\}_{t \in \mathbb{Z}}$ is an i.i.d. random variable sequence with zero mean and unit variance.

3.1 Continuous Time Evolutionary Wavelet Spectrum

The continuous time evolutionary wavelet spectrum gives a location-scale decomposition of the spectral power of a continuous time locally stationary wavelet process.

Definition 3. The **Continuous Time Evolutionary Wavelet Spectrum**, S , of a locally stationary wavelet process $X(t)$, with respect to the wavelet family ψ , is defined by

$$dS(u, v) = \mathbb{E} [|W(u, v)L(du, dv)|^2], \quad (20)$$

for all scales $u \in \mathbb{R}^+$ and times $v \in \mathbb{R}$.

As we assume that L is a homogeneous Lévy basis, in general we have

$$S(u, v)dudv = |W(u, v)|^2 dudv, \quad (21)$$

and so can write

$$S(u, v) = |W(u, v)|^2. \quad (22)$$

Further, Definition 1(b) implies that, for all scales $u \in \mathbb{R}^+$ and times $v \in \mathbb{R}$,

$$\int_0^\infty S(u, v)du < \infty. \quad (23)$$

Since $W(u, \cdot)$ is Lipschitz continuous and bounded for all $u \in \mathbb{R}^+$, $S(u, \cdot)$ is also Lipschitz continuous with Lipschitz constant $\kappa(u)$.

Example 1 — continued. For Haar MA(α) processes we have that

$$dS(u, v) = \mathbb{E} [|W(u, v)\delta_\alpha(du)G(dv)|^2] = \delta_\alpha(du)dv \quad (24)$$

and hence the Haar MA(α) evolutionary wavelet spectrum is given by

$$S(u, v) = \delta_\alpha(u), \quad (25)$$

for all $v \in \mathbb{R}$, where u, α are as above and where we permit a slight abuse of notation as the Dirac delta function is not continuous with respect to Lebesgue measure.

3.2 Continuous Time Local Autocovariance

[9] show that the autocovariance of a locally stationary wavelet process has a wavelet representation, known as the local autocovariance. We investigate continuous time versions and begin with continuous time autocorrelation wavelets, see [35].

Definition 4. (Continuous Time Autocorrelation Wavelets). Let $u, x \in \mathbb{R}^+$ and $\tau \in \mathbb{R}$. The autocorrelation wavelets are defined by

$$\Psi(u, \tau) = \int_{-\infty}^\infty \psi(u, v)\psi(u, v - \tau)dv \quad (26)$$

and the corresponding inner product kernel is given by

$$A(u, x) = \int_{-\infty}^\infty \Psi(u, y)\Psi(x, y)dy. \quad (27)$$

Definition 5. (Local Autocovariance). For time $t \in \mathbb{R}$ and lag $\tau \in \mathbb{R}$, the local autocovariance is defined by

$$c(t, \tau) = \int_0^\infty S(u, t) \Psi(u, \tau) du, \quad (28)$$

where $S(u, t)$ and $\Psi(u, \tau)$, $u \in \mathbb{R}^+$, are the continuous time evolutionary wavelet spectrum and autocorrelation wavelets, respectively.

The usual local autocovariance function applied to continuous time locally stationary wavelet processes is given by

$$c_X(t, \tau) = \text{cov}[X(t), X(t + \tau)] = \mathbb{E}[X(t)X(t + \tau)], \quad (29)$$

as $X(t)$ has zero mean. This local autocovariance can also be written in terms of the evolutionary wavelet spectrum and the underlying wavelets of the process by

$$c_X(t, \tau) = \int_0^\infty \int_{-\infty}^\infty S(u, t + v) \psi(u, v) \psi(u, v - \tau) dv du. \quad (30)$$

See Supplementary Materials Section D Proposition 1 for proof. Comparing (28) and (30), if the process were stationary, then we would have $S(u, t + v) = S(u, t)$ and the two expressions would be equivalent everywhere. Due to the presence of the wavelet terms in the integral above, the only information in an interval centered at t , of length which is at most equal to the width of the wavelet, contributes to $c(t, \tau)$. This means that at each $t \in \mathbb{R}$, in order to compute the local autocovariance, we are assuming that the spectrum is approximately constant in an interval centered around t , which is consistent with the concept of local stationarity. We note also that as u increases, this interval also becomes wider. The next proposition establishes a bound on the maximum difference between the two expressions (28) and (30).

Proposition 1. Let $\{X(t)\}_{t \in \mathbb{R}}$ be a continuous time locally stationary wavelet process, $c_X(t, \tau)$ be its autocovariance function and $c(t, \tau)$ its local autocovariance. Then,

$$|c_X(t, \tau) - c(t, \tau)| \leq \theta(\tau) \quad (31)$$

where

$$\theta(\tau) = \left| \int_0^\infty \kappa(u) \int_{-\infty}^\infty |v| \psi(u, v) \psi(u, v - \tau) du dv \right| \quad (32)$$

and $\kappa(u)$ is the Lipschitz constant function for the evolutionary wavelet spectrum S .

When $X(t)$ is stationary, the local autocovariance $c(t, \tau)$ and the autocovariance $c_X(t, \tau)$ are equivalent since the amplitude function W is constant and consequently the Lipschitz constant function $\kappa(u)$ is equal to zero everywhere. More generally, in regions where the process is fully stationary, $c_X(t, \tau)$ and $c(t, \tau)$ are equivalent for some lags.

The bound in Proposition 1 can be inefficient as it does not depend on t . The more stationary $X(t)$ is in a given region, the closer $c(t, \tau)$ and $c_X(t, \tau)$ will be. If the spectrum S admits a Taylor series representation, for each $u \in \mathbb{R}^+$ we could write

$$S(u, t + v) \approx S(u, t) + v \frac{\partial S}{\partial v}(u, t) + o(v^2), \quad (33)$$

for v in some interval around t whose length depends on u . Using this expansion and ignoring higher order terms, we can write

$$|c_X(t, \tau) - c(t, \tau)| \approx \left| \int_0^\infty \frac{\partial S}{\partial v}(u, t) \int_{-\infty}^\infty v \psi(u, v) \psi(u, v - \tau) du dv \right|. \quad (34)$$

Although not a proper bound, this now depends on t and provides a better description of the discrepancy between the two quantities from a more local perspective.

Remark 2. A comparison of the local and standard autocovariance functions on a simple example can be found in the Supplementary Materials Section C.

From the local autocovariance we can also define the local autocorrelation as follows.

Definition 6. (Local Autocorrelation). Let $\sigma^2(t) = c(t, 0)$ be the local variance of the process $X(t)$. Then the local autocorrelation is defined as $\rho(t, \tau) = \sigma^{-2}(t) c(t, \tau)$, where $c(t, \tau)$ is the local autocovariance from above.

Example 1 - continued. For the Haar MA(α) processes, we have

$$c(t, \tau) = \Psi(\alpha, \tau) = c_X(t, \tau), \quad (35)$$

where Ψ is the Haar autocorrelation wavelet, see Supplementary Materials Section B. Since Haar MA processes are stationary, the local and standard autocovariance functions are equivalent. Further, $\rho(t, \tau) = c(t, \tau)$, since $\Psi(\alpha, 0) = 1$, as shown next. To conclude this section we list some useful properties of autocovariance wavelets and the inner product kernel.

Proposition 2. Let $\Psi(u, \tau)$, $u \in \mathbb{R}^+$, denote the autocorrelation wavelets and let $\Psi(\tau) = \Psi(1, \tau)$. Then, for all $u \in \mathbb{R}^+$:

- (a) $\Psi(u, \tau)$ is symmetric as a function of τ , i.e. $\Psi(u, \tau) = \Psi(u, -\tau)$,
- (b) $\Psi(u, 0) = 1$,
- (c) $\Psi(u, \tau) = \Psi(\tau/u)$,
- (d) The Fourier transform of $\Psi(u, t)$ as a function of t is $\hat{\Psi}(u, \omega) = u|\hat{\psi}(u\omega)|^2$,
- (e) $\int_{-\infty}^{\infty} \Psi(u, \tau) d\tau = 0$.

Proposition 3. The inner product kernel A is continuous, symmetric and non-negative definite. Furthermore, for all $b > 0$ and $x, y \in \mathbb{R}^+$,

$$A(bx, by) = bA(x, y). \quad (36)$$

For examples of autocorrelation wavelet functions and inner product kernels, see Supplementary Materials Section B.

3.3 Relationship between the (wavelet) Periodogram and Spectrum

We now define the raw wavelet periodogram and evolutionary wavelet spectrum. First, we need to define process wavelet coefficients.

Definition 7. (Wavelet Coefficients). Let $u \in \mathbb{R}^+$ and $v \in \mathbb{R}$ be scale and location respectively and define the wavelet coefficients $d(u, v)$ of the process $X(t)$ in terms of the wavelet basis ψ by

$$d(u, v) = \int_{-\infty}^{\infty} X(t)\psi(u, t - v)dt. \quad (37)$$

Definition 8. (Raw Wavelet Periodogram). Let $u \in \mathbb{R}^+$ and $v \in \mathbb{R}$ be scale and location and define the wavelet periodogram by

$$I(u, v) = |d(u, v)|^2, \quad (38)$$

where $d(u, v)$ are the wavelet coefficients of the process $X(t)$. Define the notation $\beta(u, v) = \mathbb{E}[I(u, v)]$, which turns out to be useful.

The following theorem establishes a relationship between the expected value of the raw wavelet periodogram and an integral involving the evolutionary wavelet spectrum and inner product kernel, paralleling and extending the one of [9].

Theorem 1. Let $I(u, v)$ be the raw wavelet periodogram of the locally stationary wavelet process $X(t)$, $S(u, v)$ its corresponding evolutionary wavelet spectrum and $A(u, x)$ the inner product kernel. Then

$$\left| \beta(u, v) - \int_0^{\infty} S(x, v) A(u, x) dx \right| \leq \Omega(u), \quad (39)$$

where $\beta(u, v) = \mathbb{E}[I(u, v)]$ and

$$\Omega(u) = \left| \int_0^{\infty} \kappa(x) \int_{-\infty}^{\infty} |y| \int_{-\infty}^{\infty} \int_{-\infty}^{\infty} \psi(x, t - y)\psi(x, s - y)\psi(u, t)\psi(u, s) dt ds dy dx \right|. \quad (40)$$

As previously, following Proposition 1, if $X(t)$ is stationary, then the two terms on the left hand side of (39) are equivalent.

The expectation of the raw wavelet periodogram can also be written as

$$\beta(u, v) = \int_0^{\infty} \int_{-\infty}^{\infty} S(x, y + v) \int_{-\infty}^{\infty} \int_{-\infty}^{\infty} \psi(x, t - y)\psi(x, s - y)\psi(u, t)\psi(u, s) dt ds dy dx, \quad (41)$$

where $\beta(u, v)$ is defined in Theorem 1. This can be viewed as approximating $S(u, t + v)$ with $S(u, t)$ at a local level. As S is assumed to vary slowly in time, $\Omega(u)$ will generally be small. We could also use the Taylor expansion of $S(u, v + t)$ again to obtain an expression for the local discrepancy, however for brevity we omit this here.

Remark 3. Equations (40) and (41), contain expressions resembling that of the cross-scale autocorrelation wavelets in the discrete setting, which can be found in [36].

The above theorem motivates the following definition:

Definition 9. (Inner Product Operator) Let $f \in L^2(\mathbb{R}^+)$. Then the inner product operator is a linear integral operator $T_A : L^2(\mathbb{R}^+) \mapsto L^2(\mathbb{R}^+)$ defined by

$$(T_A f)(x) = \int_0^\infty A(x, y) f(y) dy, \quad (42)$$

where $A(x, y)$ denotes the inner product kernel.

Theorem 1 and Definition 9 suggest that one could approximate $\beta(u, v)$ by

$$\beta(u, v) \approx \int_0^\infty S(x, v) A(u, x) dx = \{T_A S(\cdot, v)\}(u). \quad (43)$$

Therefore, given $\beta(u, v)$ we could invert the above linear integral equation to obtain an estimate \hat{S} of the evolutionary wavelet spectrum. We now show how this could be done using the properties of the inner product kernel and Mercer's theorem [30]: this is a key difference with the earlier discrete time version in [9].

Since T_A has a continuous symmetric kernel, it is compact, bounded and self-adjoint. Further, we can show:

Proposition 4. Let T_A be the linear integral operator from Definition 9. Then T_A has trivial null space, i.e. $N(T_A) = \{f \in L^2(\mathbb{R}^+) : T_A f = 0\} = \{0\}$.

Following discussion in Section 2, since the inner product kernel is continuous, symmetric and non-negative definite we can apply Mercer's theorem [30] to obtain a decomposition of A of the form

$$A(x, y) = \sum_{n=1}^\infty \lambda_n \varphi_n(x) \varphi_n(y), \quad (44)$$

where λ_n and φ_n are the eigenvalues and eigenfunctions of T_A . Hence, we can write

$$(T_A f)(x) = \sum_{n=1}^\infty \lambda_n \langle \varphi_n, f \rangle \varphi_n(x). \quad (45)$$

Since T_A is self-adjoint, this allows us to obtain a solution (or estimate)

$$\hat{S}(u, t) = \sum_{n=1}^\infty \lambda_n^{-1} \langle \beta(\cdot, t), \varphi_n(\cdot) \rangle \varphi_n(u), \quad (46)$$

to the linear integral equation (43), for all $u \in \mathbb{R}^+$ and $t \in \mathbb{R}$, which is unique, as we showed earlier that $N(T_A) = \{0\}$.

The evolutionary wavelet spectral estimate (46) can be used to obtain an estimate of the local autocovariance using (28). Further, the ability to invert T_A also permits us to invert (28) to obtain a representation of the spectrum in terms of the local autocovariance as follows:

Theorem 2. Let $c(z, \tau)$ be the local autocovariance of a continuous time locally stationary wavelet process. Then the evolutionary wavelet spectrum can be written as

$$S(u, z) = \sum_{n=1}^\infty \lambda_n^{-1} \varphi_n(u) \int_{-\infty}^\infty c(z, \tau) \langle \Psi(\cdot, \tau), \varphi_n(\cdot) \rangle d\tau \quad (47)$$

where Ψ is autocovariance wavelet and λ_n and φ_n are the eigenvalues and eigenvectors of the inner product operator T_A from Definition 9.

It is crucial to note that we have, so far, ignored the fact that generally one does not work directly with $\beta(u, v)$, but rather with a sample, or in some cases a set of samples, of the locally stationary wavelet process $X(t)$, which could then be used to obtain an estimate of $\beta(u, v)$. This, of course, introduces some noise into the linear integral equation. To address this problem, regularisation methods such as the spectral cut-off method discussed in Section 2 can be employed.

We now consider the practical situation where we only have access to a discrete sample of points and focus on techniques to estimate quantities from these.

4 Implementation of Spectral and Autocovariance Estimators

In practice, one typically has access to a discrete and finite realisation of the process, rather than the entire sample path. Therefore, estimation of spectral and autocovariance quantities requires adaptations of previous section's framework. To begin, we provide a new definition of locally stationary wavelet processes in continuous time, reintroducing a sequence of stochastic processes and the concept of rescaled time.

Definition 10. (Discretized Continuous Time Locally Stationary Wavelet Process). A sequence of stochastic processes $\{X_T(t)\}_{t \in \mathcal{T}}$ indexed by T , where $\mathcal{T} = \{t_0, t_1, \dots, t_n\}$ such that $0 = t_0 < t_1 < \dots < t_{n-1} < t_n = T$, is said to be a discretized continuous time locally stationary wavelet processes if it can be expressed in the form

$$X_T(t) = \int_0^{J_\psi(T)} \int_{-\infty}^{\infty} w_T(u, v) \psi(u, t - v) L(du, dv), \quad (48)$$

where L is a square-integrable homogeneous Lévy basis with $\mathbb{E}[L(A)] = 0$ and $\mathbb{E}[L(A)^2] = \text{Leb}(A)$ for all $A \in \mathcal{B}_b(\mathbb{R}^+ \times \mathbb{R})$, $\{\psi_{u,v}(x), u \in \mathbb{R}^+, v \in \mathbb{R}\}$ is a continuous wavelet family as defined above, $w_T \in L^2(\mathbb{R}^+, \mathbb{R})$, $T \in \mathbb{R}^+$, is a sequence of location-scale varying amplitude functions and $J_\psi(T)$ is an increasing function which depends on the wavelet family ψ and determines the widest scale to include. Further, for each fixed $u \in \mathbb{R}^+$, there exists a function $W(u, \cdot) : (0, 1) \mapsto \mathbb{R}$ such that:

- (a) For each fixed $u \in \mathbb{R}^+$, $W(u, \cdot)$ is a Lipschitz continuous function with Lipschitz constant $K(u)$, where the Lipschitz constant function K is uniformly bounded,

$$\int_0^\infty uK(u)du < \infty. \quad (49)$$

- (b) For each fixed $z \in (0, 1)$, $W(\cdot, z)$ satisfies

$$\int_0^\infty |W(u, z)|^2 du < \infty. \quad (50)$$

- (c) For each fixed $u \in \mathbb{R}^+$ there exists a constant $C(u)$ such that for each $T \in \mathbb{R}^+$

$$\sup_{k \in \mathbb{R}} \left| w_T(u, v) - W\left(u, \frac{v}{T}\right) \right| \leq \frac{C(u)}{T} \quad (51)$$

and

$$\int_0^\infty C(u) du < \infty. \quad (52)$$

Model Interpretation: We have reintroduced the concept of rescaled time, as this allows us to model the local structure of the process more accurately as we gather increasing amounts of data. However, unlike the discrete case, we rescale the process, assuming that the first and last data points correspond to times 0 and T respectively. The function $J_\psi(T)$ determines the maximum scale that contributes to the process and it depends on the length of the available data T . As we gather more data and T increases, we can include increasingly coarser scales in the model and thus it makes sense for $J(T)$ to be an increasing function of T .

We now redefine the evolutionary wavelet spectrum for the discretized setting:

Definition 11. The (Discretized) Evolutionary Wavelet Spectrum of the discretized locally stationary wavelet process, $X_T(t)$, with respect to ψ is defined by

$$dS(u, z) = \mathbb{E} \left[|W(u, z)L(du, dv)|^2 \right] \quad (53)$$

for all $u \in \mathbb{R}^+$ and $z = v/T \in (0, 1)$.

As before, we can write

$$S(u, z) = |W(u, z)|^2, \quad (54)$$

for $z = v/T \in (0, 1)$. Further, Definition 10 (b) and (c), imply that, for each fixed $z \in (0, 1)$,

$$\int_0^\infty S(u, z) du < \infty \quad \text{and} \quad S(u, z) = \lim_{T \rightarrow \infty} |w_T(u, v)|^2, \quad (55)$$

for all $u \in \mathbb{R}^+$ and $v \in \mathbb{R}$.

The local autocovariance and autocorrelation remain as before, except that we replace t with its rescaled version z , as was done for the evolutionary wavelet spectrum above. To emphasize the dependence on T , we now denote the autocovariance by $c_{X_T}(t, \tau)$.

Proposition 1 above highlighted the discrepancy between the ‘regular’ autocovariance $c_X(t, \tau)$ from (29) and the ‘wavelet’ autocovariance $c(t, \tau)$ from (28) for the non-discretized process with equality in the stationary case. However, in the discretized case, the autocovariances become close asymptotically, as shown by the following.

Proposition 5. *Let $\{X_T(t)\}_{t \in \mathcal{T}}$ be a locally stationary wavelet process, $c_{X_T}(t, \tau)$ its autocovariance function, $c(z, \tau)$ the local autocovariance and $z = t/T$. Then we obtain the following bound*

$$|c_{X_T}(t, \tau) - c(z, \tau)| < O(T^{-1}) \quad (56)$$

In other words, the autocovariance converges to the local autocovariance as $T \rightarrow \infty$.

4.1 Estimation Theory

We redefine the wavelet coefficients and raw wavelet periodogram for discrete data and then show how we can estimate the spectrum in practice.

Definition 12. (Wavelet Coefficients). For $u \in (0, J_\psi(T)]$ and $v \in \mathcal{T}$, the wavelet coefficients of the process $X_T(t)$ are defined by

$$d(u, v) = \int_{-\infty}^{\infty} X_T(t) \psi(u, t - v) dt. \quad (57)$$

Given observations at times $0 = t_0 < t_1 < \dots < t_{n-1} < t_n = T$, we approximate (57) above by

$$d(u, v) \approx \frac{1}{2} \sum_{i=1}^n \{X_T(t_i) \psi(u, t_i - v) + X_T(t_{i-1}) \psi(u, t_{i-1} - v)\} \Delta t_i, \quad (58)$$

where $\Delta t_i = t_i - t_{i-1}$. The higher the average sampling rate, and therefore the more data we have from 0 to T , then the better the approximation.

Definition 13. (Raw Wavelet Periodogram). For $u \in (0, J_\psi(T)]$ and $z \in (0, 1)$, with $z = v/T$, $v \in \mathcal{T}$, the raw wavelet periodogram is defined as

$$I(u, z) = I\left(u, \frac{v}{T}\right) = |d(u, v)|^2 = |d(u, zT)|^2, \quad (59)$$

where $d(u, v)$ are the wavelet coefficients of the process $X(t)$.

This leads us to the following result:

Theorem 3. *Let $I(u, z)$ be the raw wavelet periodogram of the locally stationary wavelet process $X_T(t)$, $S(u, z)$ its corresponding evolutionary wavelet spectrum and $A(u, x)$ the inner product kernel. Then*

$$\left| \beta(u, z) - \int_0^{J_\psi(T)} S(x, z) A(u, x) dx \right| \leq O(T^{-1}), \quad (60)$$

for all $u \in \mathbb{R}^+$ and $z \in (0, 1)$.

Equation (60) suggests estimating spectrum, S , by solving the linear integral equation

$$\beta(u, v) = \int_0^{J_\psi(T)} S(x, z) A(u, x) dx. \quad (61)$$

by using estimates of $\beta(u, v)$ denoted by $\hat{\beta}(u, z)$, which we elaborate on below in Section 4.2. To obtain an estimate of the spectrum, we can reformulate (61) as a minimisation problem to minimise the discrepancy

$$\Delta S = \left| \int_0^{J_\psi(T)} S(x, z) A(u, x) - \hat{\beta}(u, z) \right|^2. \quad (62)$$

In order to guarantee the non-negativity of the evolutionary wavelet spectrum, we employ the asymmetric version of [32] iterative algorithm, described at the end of Section 2. To do so, we choose a suitable value of $\mu_1 = \mu > 0$, while setting $\mu_2 = \infty$. The thresholding equation (13) can then be reformulated as

$$S_{\mu,1}(x) = \begin{cases} x - \frac{\mu}{2}, & \text{if } x \geq \frac{\mu}{2}, \\ 0, & \text{if } x < \frac{\mu}{2}, \end{cases} \quad (63)$$

for some $\mu > 0$. We can then apply the iterative scheme (11) to obtain an evolutionary wavelet spectrum estimate \hat{S} .

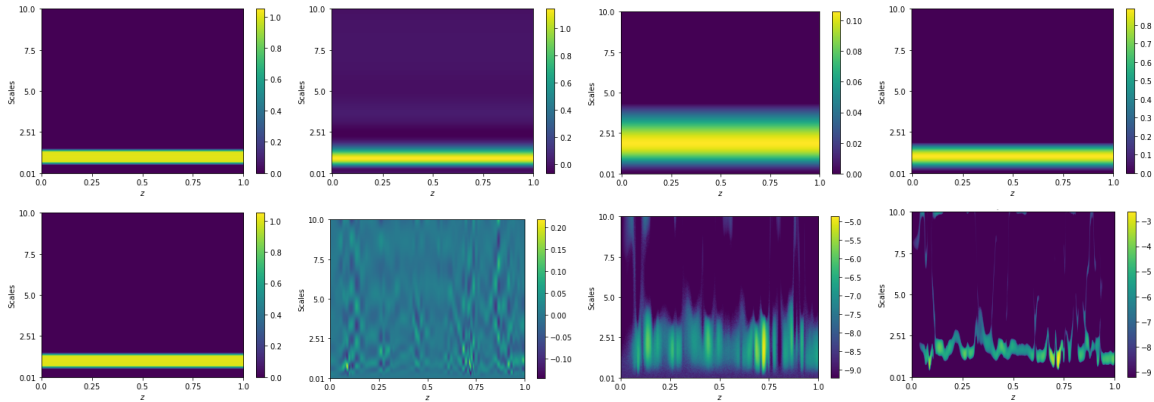


Figure 1: A comparison of Tikhonov regularisation against [32] iterative algorithm when $\beta(u, z)$ is known (top row) and when it is estimated from the data, in this case by setting $\hat{\beta}(u, z) = I(u, z)$ (bottom row). From left to right: original spectrum, solution using Tikhonov regularisation, solutions from running the [32] iterative algorithm for 100 and 10000 iterations.

4.2 Practical Considerations

In practice, we work with an estimate of $\beta(u, z)$, which we denote $\hat{\beta}(u, z)$. In most situations, we only have one realisation of the process, $X_T(t)$, and thus our best estimate would simply be $\hat{\beta}(u, z) = I(u, z)$. However, there are situations where we may have access to replicated time series, see [37] for example, and can set

$$\hat{\beta}(u, z) = n^{-1} \sum_{i=1}^n I_i(u, z), \quad (64)$$

where n is the number of replicates and $I_i(u, z)$ denotes the raw wavelet periodogram for the i -th realisation.

When we can access the actual (theoretical) value of $\beta(u, z)$, Tikhonov regularisation is the natural choice for inverting (61), both in terms of accuracy and computational efficiency (see top row of Figure 1). However, as soon as we work with estimates, the performance of Tikhonov regularisation deteriorates and no longer guarantees the non-negativity of the evolutionary wavelet spectrum. In such cases, the [32] iterative thresholding algorithm described earlier is our preferred choice, as it remains robust against noise contamination (see second figure from the left in the bottom row of Figure 1).

We observe that, in general, convergence of information at finer scales tends to take longer. One explanation is that, given the same level of information at coarser at finer scales, the wavelet coefficients at coarser scales tend to be larger than those at finer ones. Furthermore, information at wider scales tends to exhibit higher variability compared to the same information at finer scales. For observations at coarser scales, the range of scales that are likely to have large coefficients is wider, growing logarithmically with the scale width. To address this effect, we apply level-dependent universal wavelet smoothing to the raw wavelet periodogram before transforming to the evolutionary wavelet spectrum, see [38, 18] for further details.

4.3 Non-Stationary Haar Moving Average Example

We now apply our methods to a set of non-stationary Haar moving average samples. The true underlying evolutionary wavelet spectrum is displayed the upper left part of Figure 2 (for the full functional specification see Supplementary Materials Section D). We also display a sample drawn from this spectrum, as well as the theoretical local autocovariance and autocorrelation.

We draw 1000 realisations, $X_T(t)$, of a process with the Haar MA evolutionary wavelet spectrum and compute an estimate of $\beta(u, z)$ using (64) for $n = 1, 10, 100$ and 1000. In each case, we then use the [32] iterative algorithm to compute an evolutionary wavelet spectral estimate. The results of this running 100, 1000 and 10000 algorithm iterations are displayed in Figure 3. As expected, results improve as we increase both the number of samples used to compute (64) and the number of iterations in the [32] iterative thresholding algorithm. As mentioned in the practical considerations, we observe that finer scale information requires a larger number of iterations to become as visible in the estimate as information at larger scales. Additionally, we notice that spectral information tends to deviate more from its true value at larger scales, which aligns with the comments made in Supplementary Materials Section C.

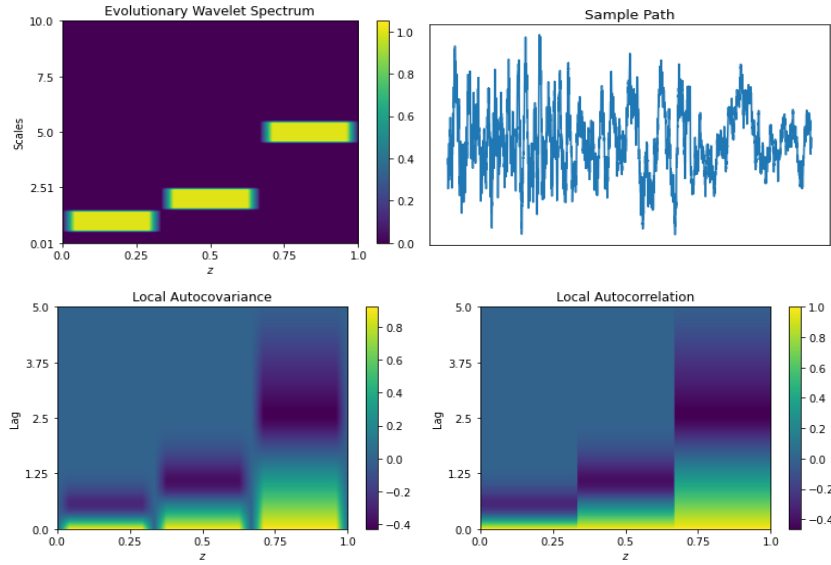


Figure 2: From left to right, top to bottom: the theoretical evolutionary wavelet spectrum, a sample realisation and the theoretical local autocovariance and autocorrelation functions for the non-stationary Haar moving average process.

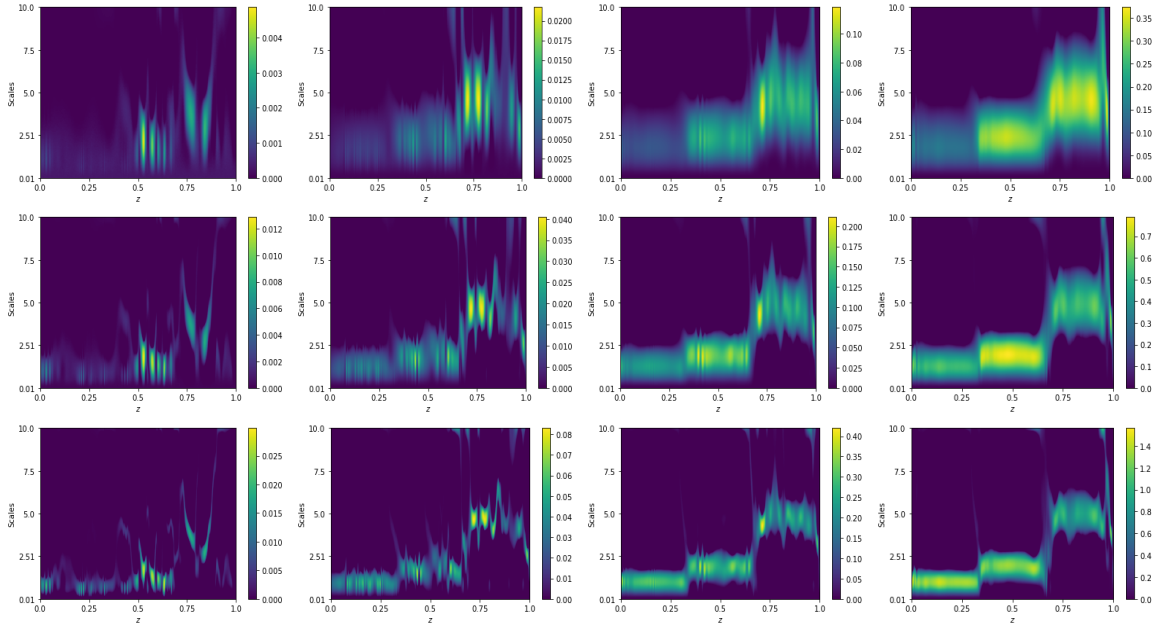


Figure 3: Estimates of the evolutionary wavelet spectrum spectrum. From left to right: $\hat{\beta}(u, z)$ estimated using 1, 10, 100 and 1000 samples. From top to bottom: results from running the iterative thresholding algorithm for 100, 1000 and 10000 iterations.

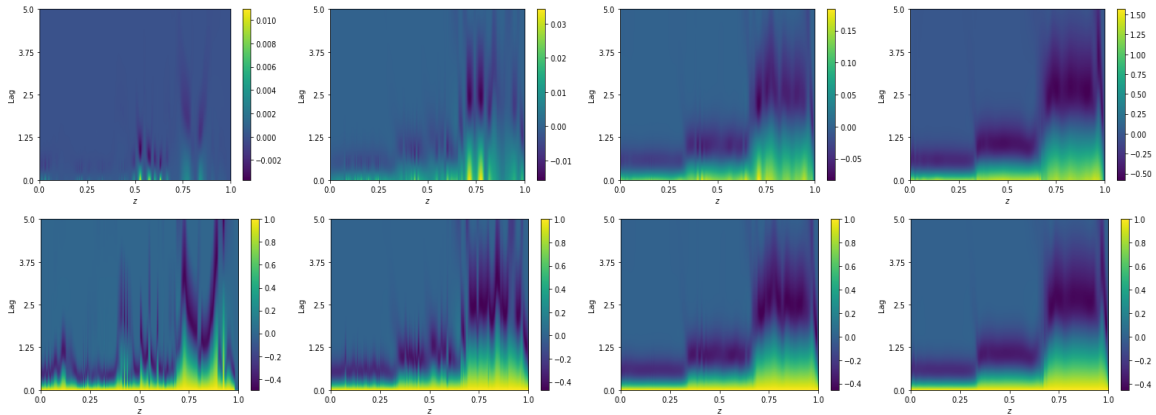


Figure 4: Local autocovariance (top row) and autocorrelation (bottom row) estimates for the non-stationary Haar moving average process using evolutionary wavelet spectral estimates obtained from running the [32] iterative algorithm for 10000 iterations. The columns are sorted in ascending order of the number of samples used to estimate $\hat{\beta}(u, z)$.

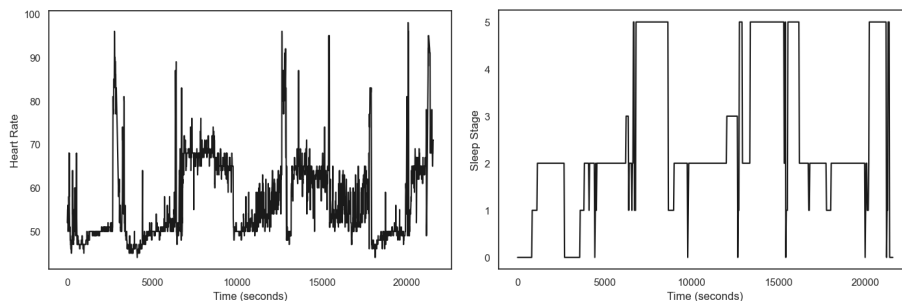


Figure 5: Heart rate of a sleeping individual (left) and corresponding sleep labels (right). Data obtained from [40]

We now use our evolutionary wavelet spectrum estimates and (28) to obtain a local autocovariance estimate, and thence an estimate of the local autocorrelation and both shown in Figure 4. For this purpose, we only use our evolutionary wavelet spectral estimate which was obtained by running the [32] iterative algorithm for 10000 iterations.

Once again, as anticipated, the results improve as the number of samples used to compute $\hat{\beta}(u, z)$ increase. Even when only one sample is employed, it is still possible to distinguish between different frequency regions, although this distinction is more apparent in the local autocorrelation estimate compared to the local autocovariance estimate. When a smaller number of samples are used, all estimates, including those of the evolutionary wavelet spectrum, display a higher degree of variability. Therefore, it may be beneficial to further investigate more appropriate smoothing techniques, an avenue which we leave for future research.

5 Application to Heart Rate and Sleep Stage Data

We now apply our methods to study the heart rate of a sleeping individual. The data in our study here are irregularly spaced and so the discrete time methods from [9] simply cannot be used. Existing methods [11] for dealing with irregularly-spaced data in this setting are computationally demanding and of poor quality (as they produce estimates of a very different nature to the underlying spectral quantity we want to estimate). Our new methods are the only ones to our knowledge that can produce a genuine estimate in reasonable time for irregularly-spaced data.

[39] collected data for a study to attempt to predict different sleep stages based on heart rate recordings obtained from wearable devices during sleep. The data are available at [40]. The heart rate and sleep stages of several individuals were recorded and we selected one for our analyses. The sleep stages are labelled 0 to 5, representing progressively deeper stages of sleep. Specifically, stage 0 corresponds to wakefulness, stages 1 to 3 correspond to non-rapid eye movement (NREM) sleep stages 1 to 3, and stage 5 corresponds to REM sleep. Figure 5 shows the heart rate and sleep stage of the chosen individual, which clearly exhibits non-stationary behaviour.

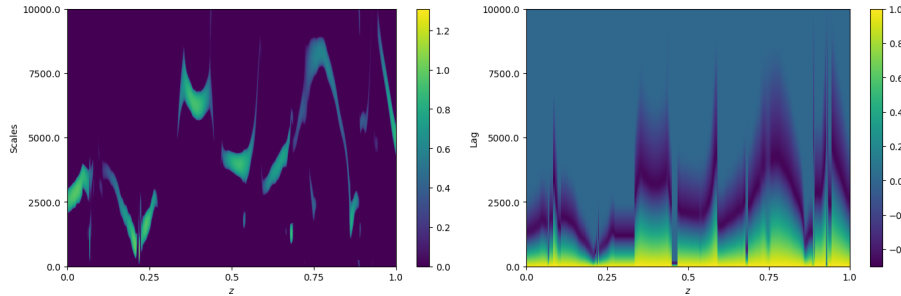


Figure 6: Estimates of the evolutionary wavelet spectrum (left) and local autocorrelation (right) for the Haar locally stationary wavelet model fitted to the heart rate data.

We fit models using Haar wavelets as the underlying wavelet functions, with scales ranging from 1 to 10000 and symmetric boundary conditions. To compute an evolutionary wavelet spectral estimate, we employed the [32] iterative algorithm, from which we then obtained an estimate of the local autocorrelation function. Prior to estimating the evolutionary wavelet spectrum smoothing techniques were also applied to the raw wavelet periodogram, as described above.

Figure 6 displays the estimates. The evolutionary wavelet spectral estimate, is concentrated primarily at coarser scales in regions where the heart rate corresponds to deeper sleep stages, such as the NREM stage. We can clearly see three distinct peaks, which seem to align with those in the sleep stage labels plot, although the rightmost one is less visible, possibly due to boundary effects or other noise sources. A similar relationship can be observed when viewing the local autocorrelation estimate, although this is somewhat less clear. This suggests that spectral information at larger scales corresponds to deeper sleep stages, whereas information appearing at finer scales corresponds to lighter sleep.

The above suggests that such methods can provide valuable insight into the analysis of (sampled) irregularly-spaced time series, in this case heart rate and sleep stage data. However, one of the biggest limitations is that we only had one realisation in order to estimate $\beta(u, z)$ and, in turn, the evolutionary wavelet spectrum and local autocovariance. If multiple realisations of this time series were available, better estimates could be formed.

6 Conclusions and Future Work

This article introduces continuous time locally stationary wavelet processes along with the associated continuous time evolutionary wavelet spectra and local autocovariance. Our new methods are ideally suited for the modelling and analysis of irregularly-spaced time series data or regularly-spaced time series subject to missingness. We have introduced rigorous theory using homogeneous Lévy bases to embed our new continuous time processes and associated quantities. A key contribution is the application of the [32] iterative algorithm for solving the key linear integral equation to obtain positive spectral quantities and also deal with noise. The novel methods developed here permit accurate estimates the evolutionary wavelet spectrum within a reasonable computational time-frame. Further, our evolutionary wavelet spectrum is inherently defined across a continuous spectrum of scales, thereby offering a more comprehensive representation of the underlying frequency information for time series, irregular or not.

Our new continuous time locally stationary wavelet process work throws up several interesting avenues for future work. First, one promising direction would be the development of improved smoothing techniques for the raw wavelet periodogram, to enable more accurate and reliable estimation of the evolutionary wavelet spectrum and local autocovariance. This is particularly relevant for processes that exhibit significant spectral power at larger scales.

Second, it would be useful to investigate the impact of discrete approximations on continuous time models, particularly in relation to aliasing. The study on the effects of aliasing in the context of locally stationary wavelet processes has shown promise in detecting its absence [20, 21]. Extending these methods to the continuous time models developed in this article could yield further insights into such behaviours, which only work because of their non-stationarity.

Other directions for future work could also include the development of alternative approaches or algorithms for estimating the evolutionary wavelet spectrum, and related quantities or exploring applications of these models in various fields such as finance, economics, healthcare or physics.

Acknowledgements: We would like to thank Almut Veerart for helpful discussions and feedback.

Proofs and Code Availability: Proofs can be found in Supplementary Materials Section E. The code can be found at: <https://github.com/henrypalasciano/CLSWP>

References

- [1] P. J. Brockwell and R. A. Davis. *Time Series: Theory and Methods*. Springer, New York, 1991.
- [2] D. B. Percival and A. T. Walden. *Spectral Analysis for Univariate Time Series*. Cambridge University Press, Cambridge, 2020.
- [3] A. J. Boness, A. H. Chen, and S. Jatusipitak. Investigations of nonstationarity in prices. *J. Bus.*, 47(4):518–537, October 1974.
- [4] G. Livan, J. Inoue, and E. Scalas. On the non-stationarity of financial time series: impact on optimal portfolio selection. *J. Stat. Mech-Theory E*, 2012(07):P07025, July 2012.
- [5] T. A. Schmitt, D. Chetalova, R. Schäfer, and T. Guhr. Non-stationarity in financial time series: Generic features and tail behavior. *Europhysics Letters*, 103(5), September 2013.
- [6] P. Fryzlewicz. Modelling and forecasting financial log-returns as locally stationary wavelet processes. *J. Appl. Stat.*, 32:503–528, 07 2005.
- [7] M. B. Priestley. *Spectral Analysis and Time Series, Volumes I and II*. London: Academic Press, 1983.
- [8] R. Dahlhaus. Fitting time series models to nonstationary processes. *Ann. Statist.*, 25(1):1–37, February 1997.
- [9] G. P. Nason, R. von Sachs, and G. Kroisandt. Wavelet processes and adaptive estimation of the evolutionary wavelet spectrum. *J. R. Statist. Soc. B*, 62(2):271–292, 2000.
- [10] M. I. Knight and G. P. Nason. A ‘nondecimated’ lifting transform. *Stat. Comput.*, 19:1–16, Apr 2008.
- [11] M. I. Knight, M. A. Nunes, and G. P. Nason. Spectral estimation for locally stationary time series with missing observations. *Stat. Comput.*, 22:877–895, Jul 2011.
- [12] Feike C. Drost and Bas J.M. Werker. Closing the GARCH gap: Continuous time GARCH modeling. *J. Econometrics*, 74(1):31–57, 1996.
- [13] P. J. Brockwell, R. A. Davis, and Y. Yang. Continuous-time Gaussian autoregression. *Statistica Sinica*, 17(1):63–80, Jan 2007.
- [14] E. Calvello, S. Reich, and A. M. Stuart. Ensemble Kalman methods: A mean field perspective. *arXiv preprint arXiv:2209.11371*, September 2022.
- [15] L. Lucchese, M. S. Pakkanen, and A. E. D. Veraart. Estimation and inference for multivariate continuous-time autoregressive processes. *arXiv preprint arXiv:2307.13020*, July 2023.
- [16] A. Bitter, R. Stelzer, and B. Ströh. Continuous-time locally stationary time series models. *Adv. Appl. Probab.*, 55:965–998, June 2023.
- [17] R. Dahlhaus. Locally stationary processes. *Handbook of Statistics*, 30:351–413, May 2012.
- [18] G.P. Nason. *Wavelet Methods in Statistics with R*. Springer: New York, 2008.
- [19] L. Winkelmann. Forward guidance and the predictability of monetary policy: a wavelet-based jump detection approach. *J. R. Statist. Soc. C*, 65(2):299–314, 2016.
- [20] I. A. Eckley and G. P. Nason. A test for the absence of aliasing or local white noise in locally stationary wavelet time series. *Biometrika*, 105(4):833–848, 2018.
- [21] H. A. Palasciano and G. P. Nason. A test for the absence of aliasing or white noise in two-dimensional locally stationary wavelet processes. *Stat. Comput.*, 33(108), July 2023.
- [22] J.D. Romano and N.J. Cornish. Detection methods for stochastic gravitational-wave backgrounds: a unified treatment. *Living Rev. Relativ.*, 20(2):1–223, 2017.
- [23] J. Nowotarski, J. Tomczyk, and R. Weron. Robust estimation and forecasting of the long-term seasonal component of electricity spot prices. *Energ. Econ.*, 39:13–27, 2013.
- [24] L. M. de Menezes, M. A. Houllier, and M. Tamvakis. Time-varying convergence in European electricity spot markets and their association with carbon and fuel prices. *Energ. Policy*, 88:613–627, 2016.
- [25] O.E. Barndorff-Nielsen, F. Espen Benth, and A.E.D. Veraart. *Ambit Stochastics*. Springer, 2018.
- [26] B. S. Rajput and J. Rosinski. Spectral representations of infinitely divisible processes. *Probab. Theory Rel.*, 82:451–487, August 1989.
- [27] D. Applebaum. *Lévy Processes and Stochastic Calculus*. Cambridge Studies in Advanced Mathematics. Cambridge University Press, 2009.

- [28] J. Walsh. *An Introduction to Stochastic Partial Differential Equations*. In: Hannequin, P.L. (eds) École d'Été de Probabilités de Saint Flour XIV - 1984. Lecture Notes in Mathematics, vol 1180. Springer, 1986.
- [29] R. Cont and P. Tankov. *Financial Modelling with Jump Processes*. Chapman & Hall/CRC Financial Mathematics Series. CRC Press LLC, 2003.
- [30] J. Mercer. Functions of positive and negative type, and their connection with the theory of integral equations. *Philos. T. Roy. Soc. A*, 209:415–446, May 1909.
- [31] R. Kress. *Linear Integral Equations*. Applied Mathematical Sciences 82. Springer, 1999.
- [32] I. Daubechies, M. Defrise, and C. De Mol. An iterative thresholding algorithm for linear inverse problems with a sparsity constraint. *Comm. Pure Appl. Math.*, 57:1413–1457, November 2004.
- [33] S.M. Zemyan. *The Classical Theory of Integral Equations A Concise Treatment*. Springer, 2012.
- [34] I. Daubechies. *Ten Lectures on Wavelets*. Philadelphia: SIAM, 1992.
- [35] Gregory Beylkin and N. Saito. Wavelets, their autocorrelation functions, and multiresolution representations of signals. In David P. Casasent, editor, *Intelligent Robots and Computer Vision XI: Biological, Neural Net, and 3D Methods*, volume 1826, pages 39–50. International Society for Optics and Photonics, SPIE, 1992.
- [36] Rebecca Killick, Marina I. Knight, Guy P. Nason, and Idris A. Eckley. The local partial autocorrelation function and some applications. *Elec. J. Stat.*, 14(2):3268 – 3314, 2020.
- [37] P. J. Diggle and I. al Wasel. Spectral analysis of replicated biomedical time series. *J. R. Statist. Soc. C*, 46(1):31–71, 1997.
- [38] D. L. Donoho and I. M. Johnstone. Ideal spatial adaption via wavelet shrinkage. *Biometrika*, 81:425–455, 1994.
- [39] O. Walch, Y. Huang, D. Forger, and C. Goldstein. Sleep stage prediction with raw acceleration and photoplethysmography heart rate data derived from a consumer wearable device. *Sleep*, 42(12), 08 2019. zsz180.
- [40] O. Walch. Motion and heart rate from a wrist-worn wearable and labeled sleep from polysomnography. *PhysioNet*, Oct 2019.
- [41] J. Buesco and A.C. Paixao. Eigenvalue distribution of mercer-like kernels. *Math. Nachr.*, 280:935–1218, June 2007.
- [42] T. Hastie, R. Tibshirani, and J. Friedman. *The Elements of Statistical Learning*. Springer, 2009.

A - Background Materials

This section reviews some of the relevant background materials in more detail beginning with locally stationary wavelet processes in discrete time, followed by Lévy processes and bases and concludes with some useful methods for solving linear integral equations.

6.1 Review of Locally Stationary Wavelet Processes in Discrete Time

Locally stationary wavelet processes [9, 18] are time series models that have found applications in various domains, including finance [6], economics [19] aliasing detection [20, 21] and energy [23, 24]. They are constructed from discrete wavelets as follows.

Definition 14. (Discrete Wavelets). [9] Let $\{g_k\}_{k \in \mathbb{Z}}$ and $\{h_k\}_{k \in \mathbb{Z}}$ be the high and low-pass quadrature mirror filters used in the construction of the Daubechies [34] compactly supported orthogonal continuous wavelets. Let N_h be the number of non-zero elements of $\{h_k\}_{k \in \mathbb{Z}}$ and $N_j = (2^j - 1)(N_h - 1) + 1$ for scales $j \in \mathbb{N}$. Then the discrete wavelets $\psi_j = (\psi_{j,0}, \psi_{j,1}, \dots, \psi_{j,N_j-1})$ are vectors of length N_j obtained using the formulae

$$\psi_{1,n} = \sum_k g_{n-2k} \delta_{0,k} = g_n, \quad n = 0, \dots, N_1 - 1, \quad (65)$$

$$\psi_{j+1,n} = \sum_k h_{n-2k} \psi_{j,k}, \quad n = 0, \dots, N_{j+1} - 1, \quad (66)$$

where $\delta_{0,k}$ denotes the Kronecker delta.

The locally stationary wavelet processes can then be defined as follows.

Definition 15. (Locally Stationary Wavelet Process). [9] A locally stationary wavelet process is a sequence of stochastic processes $\{X_{t,T}\}_{t=0,\dots,T-1}$ ($T = 2^j$, for some $j \in \mathbb{N}$) having the following representation in the mean square sense:

$$X_{t,T} = \sum_{j=1}^{\infty} \sum_{k=-\infty}^{\infty} w_{j,k;T} \psi_{j,k-t} \xi_{j,k}, \quad (67)$$

where $\{w_{j,k;T}\}_{j \in \mathbb{N}, k \in \mathbb{Z}}$ is a set of amplitudes, $\{\psi_{j,k-t}\}_{j \in \mathbb{N}, k \in \mathbb{Z}}$ are discrete wavelets and $\{\xi_{j,k}\}_{j \in \mathbb{N}, k \in \mathbb{Z}}$ is a set of random variables with zero mean and unit variance. Furthermore, for each $j \in \mathbb{N}$ there exists a Lipschitz continuous function $W_j : (0, 1) \mapsto \mathbb{R}$ such that:

- (a) $\sum_{j=1}^{\infty} |W_j(z)|^2 < \infty$ uniformly in $z \in (0, 1)$;
- (b) the Lipschitz constants, L_j , are uniformly bounded in j and $\sum_{j=1}^{\infty} 2^j L_j < \infty$;
- (c) there exist constants $\{C_j\}_{j \in \mathbb{N}}$ such that for each T ,

$$\sup_k |w_{j,k;T} - W_j(k/T)| \leq C_j/T, \quad (68)$$

where for each j the supremum is over $k = 0, 1, \dots, T - 1$ and $\{C_j\}_{j \in \mathbb{N}}$ is such that $\sum_{j=1}^{\infty} C_j < \infty$.

The functions W_j are employed in LSW (locally stationary wavelet) models using re-scaled time, which involves scaling the process from \mathbb{N} to the unit interval $(0, 1)$. This concept, introduced by [8], is commonly employed when working with locally stationary processes. Within this framework, the limit $T \rightarrow \infty$ is interpreted as an increasing amount of information becoming available regarding the local characteristics of the process. We now present spectral quantities:

Definition 16. (Evolutionary Wavelet Spectrum). [9] The evolutionary wavelet spectrum of the locally stationary wavelet process $\{X_{t,T}\}_{t=0,\dots,T-1}$ is defined as

$$S_j(z) = |W_j(z)|^2, \quad j \in \mathbb{N}, \quad z \in (0, 1) \quad (69)$$

with respect to $\{\psi_{j,k}\}$.

The evolutionary wavelet spectrum provides a time-scale decomposition of the contribution to the variance of the process $X_{t,T}$. Note $S_j(z)$ is approximately equivalent to the variance of the process integrated over frequency band $[2^{-j}\pi, 2^{1-j}\pi]$, although the exact frequency band depends on the choice of wavelet. [20]

One of the fundamental concepts in the study of time series is that of the autocovariance of a process. Fortunately, for locally stationary wavelet processes, the autocovariance can be expressed in terms of the underlying wavelets and the evolutionary wavelet spectrum. This representation mirrors that of the autocovariance of a stationary time series in the Fourier domain,

$$c(\tau) = \int_{-\infty}^{\infty} \exp(i\omega\tau) dS(\omega). \quad (70)$$

and necessitates autocorrelation wavelets defined next.

Definition 17. (Autocorrelation Wavelets). [9] Let $j, \ell \in \mathbb{N}$ and $\tau \in \mathbb{Z}$. The autocorrelation wavelets are given by

$$\Psi_j(\tau) = \sum_k \psi_{j,k} \psi_{j,k-\tau}, \quad (71)$$

and the corresponding inner product operator is defined as

$$A_{j,\ell} = \sum_{\tau} \Psi_j(\tau) \Psi_{\ell}(\tau). \quad (72)$$

Definition 18. (Local Autocovariance). [9] The local autocovariance of the locally stationary wavelet process $\{X_{t,T}\}_{t=0,\dots,T-1}$ is defined as

$$c(z, \tau) = \sum_{j=1}^{\infty} S_j(z) \Psi_j(\tau), \quad \tau \in \mathbb{Z}, \quad z \in (0, 1). \quad (73)$$

The local autocovariance $c(z, \tau)$ is the limit of the autocovariance $c_T(z, \tau)$ of the process X_T as $T \rightarrow \infty$. [9].

We conclude this section with the definition of the raw wavelet periodogram, which is a biased estimator of the evolutionary wavelet spectrum. To obtain an unbiased estimator of the evolutionary wavelet spectrum, it is necessary to correct the raw periodogram using the inner product operator defined earlier, see [9] for further information.

Definition 19. (Raw Wavelet Periodogram). [9] The raw wavelet periodogram of the locally stationary wavelet process $\{X_{t,T}\}_{t=0,\dots,T-1}$ is defined as

$$I_{\ell,m} = d_{\ell,m}^2, \quad \ell \in \mathbb{N}, \quad m \in \mathbb{Z}, \quad (74)$$

where $\{d_{\ell,m}\}$ are the non-decimated wavelet coefficients of $X_{t,T}$ given by

$$d_{\ell,m} = \sum_{t=0}^{T-1} X_{t,T} \psi_{\ell,m-t}, \quad \ell \in \mathbb{N}, \quad m \in \mathbb{Z}. \quad (75)$$

6.2 Review of Lévy Processes

We now provide a brief overview of Lévy processes and bases, which play a crucial role in the definition of locally stationary wavelet processes in continuous time. The contents of this section draw heavily from [25, 26, 27, 28, 29]. In the following discussion, we take $(\Omega, \mathcal{F}, \mathbb{P})$ to be the underlying probability space, $(S, \mathcal{B}(S))$ to be a Borel space and denote the bounded Borel sets of $\mathcal{B}(S)$ by $\mathcal{B}_b(S)$. Definitions 20 through to Proposition 7 provide the basic underlying machinery for the construction of our continuous time locally stationary wavelet processes.

Definition 20. (Infinite Divisibility). [25, 27] Let X be a real-valued random variable. Then X is infinitely divisible if, for all $n \in \mathbb{N}$, there exist i.i.d. random variables $Y_1^{(n)}, \dots, Y_n^{(n)}$ such that $X \stackrel{d}{=} Y_1^{(n)} + \dots + Y_n^{(n)}$, where $\stackrel{d}{=}$ denotes equivalence in distribution.

Definition 21. (Lévy Process). [25, 29] A real-valued stochastic process $L = \{L(t)\}_{t>0}$ on $(\Omega, \mathcal{F}, \mathbb{P})$ is called a Lévy process if it exhibits the following properties:

- (a) $L(0) = 0$ almost surely,
- (b) L has independent increments: for any $n \in \mathbb{N}$ and any sequence of times $t_0 < t_1 < \dots < t_n$, the random variables $L(t_0), L(t_1) - L(t_0), \dots, L(t_n) - L(t_{n-1})$ are independent,
- (c) L has stationary increments: the law of $L(t+s) - L(t)$ does not depend on t ,
- (d) L is continuous in probability: $\forall \varepsilon > 0, \lim_{h \rightarrow 0} \mathbb{P}(|L(t+h) - L(t)| \geq \varepsilon) = 0$,

(e) L has càdlàg paths.

Theorem 4. (Lévy-Khintchine). [27, 25] Let X be an \mathbb{R}^n -valued random variable. Then X is infinitely divisible if there exists a vector $b \in \mathbb{R}^n$, a positive definite symmetric $n \times n$ matrix A and a Lévy measure ν on $\mathbb{R}^n \setminus \{0\}$, i.e. a measure satisfying $\int_{\mathbb{R}^n \setminus \{0\}} \max(|y|^2, 1) \nu(dy) < \infty$, such that, for all $u \in \mathbb{R}^n$,

$$\begin{aligned} \phi_X(u) &= \mathbb{E}(\exp(i\langle u, X \rangle)) \\ &= \exp i\langle b, u \rangle - \frac{1}{2} \langle u, Au \rangle + \int_{\mathbb{R}^n \setminus \{0\}} \left(e^{i\langle u, y \rangle} - 1 - i\langle u, y \rangle \mathbb{1}_{B_1(0)}(y) \right) \nu(dy), \end{aligned} \quad (76)$$

where $B_1(0)$ is the open ball of radius 1 centred at 0 and $\langle \cdot, \cdot \rangle$ denotes the inner product in \mathbb{R}^d . Conversely, any mapping of this form is the characteristic function of an infinitely divisible random variable on \mathbb{R}^n .

Since every Lévy process is infinitely divisible, its characteristic function also takes the above form. Therefore, a Lévy process can be seen as a Brownian motion with drift b interspersed with jumps of arbitrary size [27].

Definition 22. (Random Measure). [27, 25] A random measure M is a collection of real-valued random variables $\{M(A) : A \in \mathcal{B}_b(S)\}$ such that if A_1, A_2, \dots is a sequence of disjoint elements of $\mathcal{B}_b(S)$ satisfying $\bigcup_{j=1}^{\infty} A_j \in \mathcal{B}_b(S)$, then

$$M\left(\bigcup_{j=1}^{\infty} A_j\right) = \sum_{j=1}^{\infty} M(A_j), \quad (77)$$

where the right hand side converges almost surely (a.s.).

Definition 23. (Stationarity). [25] A random measure M is said to be stationary if for all $s \in S$ and any finite collection A_1, A_2, \dots, A_n of elements of $\mathcal{B}_b(S)$, the random vector $\{M(A_1 + s), M(A_2 + s), \dots, M(A_n + s)\}$ has the same law as $\{M(A_1), M(A_2), \dots, M(A_n)\}$.

Definition 24. (Lévy Basis). [25] A real valued Lévy basis on S is a collection $\{L(A) : A \in \mathcal{B}_b(S)\}$ of random variables satisfying the following properties:

(a) If A and B are disjoint subsets in $\mathcal{B}_b(S)$, then

$$L(A \cup B) = L(A) + L(B), \quad \text{a.s.} \quad (78)$$

(b) If A and B are disjoint subsets in $\mathcal{B}_b(S)$, then $L(A)$ and $L(B)$ are independent,

(c) The law of $L(A)$ is infinitely divisible for all $A \in \mathcal{B}_b(S)$.

Equivalently, we could define a Lévy basis L as an independently scattered (i.e. if A_1, A_2, \dots is a sequence of disjoint elements of $\mathcal{B}_b(S)$, then the random variables $M(A_1), M(A_2), \dots$ are independent), infinitely divisible random measure. See [25] for a proof of the equivalence between the two definitions.

Proposition 6. [25] Let L be a Lévy basis and $u \in \mathbb{R}$. Then for all $A \in \mathcal{B}_b(S)$,

$$\phi_{L(A)}(u) = \mathbb{E}[\exp\{iuL(A)\}] \quad (79)$$

$$= \exp \left\{ iu \xi^*(A) - \frac{1}{2} u^2 a^*(A) + \int_{\mathbb{R}} \left(e^{iux} - 1 - iux \mathbb{1}_{[-1,1]}(x) \right) n(dx, A) \right\} \quad (80)$$

where ξ^* is a signed measure on $\mathcal{B}_b(S)$, a^* is a measure on $\mathcal{B}_b(S)$ and $n(\cdot, \cdot)$ is the generalised Lévy measure.

Since the law of $L(A)$ for all $A \in \mathcal{B}_b(S)$ it is infinitely divisible, it is not surprising that it has a Lévy-Khintchine representation.

Definition 25. (Homogeneous Lévy Basis). [25] Let L denote a Lévy basis on $(\mathbb{R}^n, \mathcal{B}(\mathbb{R}^n))$. If ξ^* , a^* , $n(dx, \cdot)$, as defined in Proposition 6 are all absolutely continuous with respect to the Lebesgue measure and their Radon-Nikodym derivatives do not depend on $z \in S$, the L is a homogeneous Lévy basis.

Proposition 7. [25] Let L be a Lévy basis on $(\mathbb{R}^n, \mathcal{B}(\mathbb{R}^n))$. Then L is homogeneous if and only if it is stationary.

When defining continuous time locally stationary wavelet processes, we restrict our attention to homogeneous Lévy bases as the above proposition makes the concepts of homogeneity and stationarity synonymous. This is a desirable property, as we would like to control the non-stationarity of the process entirely through the deterministic amplitude functions of the process. More on this in Section 3.

Example 2 (Homogeneous Gaussian Lévy Basis). [25] Let G be a Lévy basis. If $G(A) \sim \mathcal{N}(\mu \text{Leb}(A), \sigma^2 \text{Leb}(A))$ for all $A \in \mathcal{B}(\mathbb{R}^n)$, for some $\mu \in \mathbb{R}$ and $\sigma \in \mathbb{R}^+$, then G is a homogeneous Gaussian Lévy basis. Gaussian Lévy bases are equivalent to the concept of white noise as defined in [28].

If L is a homogeneous Lévy basis on $(\mathbb{R}, \mathcal{B}(\mathbb{R}))$, then the process $(L_t)_{t \geq 0}$ with $L_t = L([0, t])$ is a Lévy process. Conversely, given a Lévy process $(L_t)_{t \geq 0}$, we can obtain a Lévy basis L by setting $L((s, t]) = L_t - L_s$. It is easy to see a similar connection between a homogeneous Gaussian Lévy basis and Brownian motion. [25]

6.3 Review of Linear Integral Equations and Regularisation Methods

Lastly, we review the relevant concepts on linear integral equations and regularisation methods. Although not strictly necessary for defining locally stationary wavelet process in continuous time, these tools will be useful when we wish to obtain an estimate of the evolutionary wavelet spectrum. The material presented in this section draws from [31, 32, 30, 33]. We denote the adjoint of a linear operator, T , by T^\dagger , its eigenvalues and eigenfunctions by λ_n and φ_n respectively, and the null space of T by $N(T)$.

Definition 26. (Integral Operator) [31] Let $S \subset \mathbb{R}^n$, $K : S \times S \mapsto \mathbb{R}$ be a continuous function and $h \in L^2(S)$. Then the linear operator $T : L^2(S) \mapsto L^2(S)$ defined by

$$(Th)(x) = \int_S K(x, y)h(y) dy, \quad x \in S, \quad (81)$$

is called an integral operator with continuous kernel K . Integral operators are compact and bounded.

We focus on linear integral equations of the first kind, given by

$$Th = f \quad (82)$$

where f and the integral operator T are known, and h is an unknown function. However, compact linear operators do not possess a bounded inverse, which can lead to problems when attempting to invert the above equation in order to obtain h .

When T is a self-adjoint compact linear operator on a Hilbert space, T has at most countably many different eigenvalues λ_n accumulating at zero. Denoting the orthogonal projections onto the eigenspaces by P_n and assuming that the sequence of non-zero eigenvalues is ordered such that $|\lambda_1| \geq |\lambda_2| \geq \dots$, we have

$$T = \sum_{n=1}^{\infty} \lambda_n P_n \quad (83)$$

in the sense of norm convergence. Under certain conditions, Mercer's theorem [30] also gives us a decomposition of the kernel:

Theorem 5. (Mercer's Theorem) [30] [41] Let T be a linear integral operator defined by

$$(Th)(x) = \int_S K(x, y)h(y) dy \quad (84)$$

where K is a continuous symmetric non-negative definite kernel. Then the kernel K can be expanded in terms of the eigenvalues λ_n and eigenfunctions φ_n of T as

$$K(x, y) = \sum_{n=1}^{\infty} \lambda_n \varphi_n(x) \varphi_n(y), \quad (85)$$

where the convergence is absolute and uniform. The non-negative definite kernel implies non-negative eigenvalues, which decay at a rate of $O(n^{-1})$.

When T is a self-adjoint linear operator, we can use the above to obtain a solution to (82) of the form

$$h = \sum_{n=1}^{\infty} \frac{1}{\lambda_n} \langle f, \varphi_n \rangle \varphi_n, \quad (86)$$

provided that $f \in N(T)^\perp$ (f belongs to the orthogonal complement of the null space of T) and

$$\sum_{n=1}^{\infty} \frac{1}{\lambda_n^2} |\langle f, \varphi_n \rangle|^2 < \infty. \quad (87)$$

If T was not self-adjoint, we have a similar expression in terms of its singular value decomposition. [31]

In practical scenarios, the presence of noise in the data f can lead to amplification of its effects on the solution due to the unboundedness of T^{-1} . This amplification is particularly pronounced for smaller eigenvalues. To address this issue, a simple often used regularisation approach is the spectral cut-off method, which replaces the solution with

$$h_\mu = \sum_{\lambda_n^2 > \mu} \frac{1}{\lambda_n} \langle f, \varphi_n \rangle \varphi_n, \quad (88)$$

for some $\mu > 0$. Alternatively, (82) can be reformulated as a minimisation problem, with the aim of minimising the discrepancy:

$$\Delta h = \|Th - f\|^2. \quad (89)$$

A pseudo-solution of the form $\tilde{h} = (T^\dagger T)^{-1} T^\dagger f$ can be obtained, assuming that T has a trivial null space ($N(T) = \{0\}$). However, the unboundedness of T^{-1} and the presence of noise can lead to difficulties. To attempt to deal with this problem, Tikhonov regularization, also known as ridge regression [42], is commonly employed. It involves minimising the constrained discrepancy

$$\Delta h = \|Th - f\|^2 + \mu \|h\|^2, \quad (90)$$

for some $\mu > 0$, in order to obtain a solution of the form

$$h_\mu = (T^\dagger T + \mu I)^{-1} T^\dagger f, \quad (91)$$

essentially penalising solutions with large norms. When T is self-adjoint, the above can be written in the form

$$h_\mu = \sum_{n=1}^{\infty} \frac{\lambda_n}{\lambda_n^2 + \mu} \langle f, \varphi_n \rangle \varphi_n \quad (92)$$

instead.

In [32], the authors propose to minimise

$$\Phi_{\mathbf{w},p}(h) = \|Th - f\|^2 + \sum_{\gamma \in \Gamma} w_\gamma |\langle h, e_\gamma \rangle|^p, \quad (93)$$

where $\{e_\gamma\}_{\gamma \in \Gamma}$ is an orthogonal basis of the Hilbert space H , $\mathbf{w} = \{w_\gamma\}_{\gamma \in \Gamma}$ is a vector of weights and $1 \leq p \leq 2$. They provide an algorithm for computing the minimiser of this functional, which we will refer to as Daubechies iterative algorithm. In particular, we will be interested in the case where $w_\gamma = \mu > 0$ for all $\gamma \in \Gamma$ and $p = 1$. In this case, the iterative scheme is given by

$$h^n = \mathbf{S}_{\mu,1}(h^{n-1} + T^\dagger(f - Th^{n-1})), \quad (94)$$

where

$$\mathbf{S}_{\mu,1}(h) = \sum_{\gamma} S_{\mu,1}(\langle h, e_\gamma \rangle) e_\gamma \quad (95)$$

and

$$S_{\mu,1}(x) = \begin{cases} x - \frac{\mu}{2}, & \text{if } x \geq \frac{\mu}{2}, \\ 0, & \text{if } |x| < \frac{\mu}{2}, \\ x + \frac{\mu}{2}, & \text{if } x \leq -\frac{\mu}{2}. \end{cases} \quad (96)$$

The authors also discuss an extension of this algorithm for cases where the positive and negative coefficients of h form the basis $\{e_\gamma\}_{\gamma \in \Gamma}$ need to be penalised differently. To do this, one replaces (96) with

$$S_{\mu_1, \mu_2, 1}(x) = \begin{cases} x - \frac{\mu_1}{2}, & \text{if } x \geq \frac{\mu_1}{2}, \\ 0, & \text{if } x < \frac{\mu_1}{2} \text{ or } x > -\frac{\mu_2}{2}, \\ x + \frac{\mu_2}{2}, & \text{if } x \leq -\frac{\mu_2}{2}, \end{cases} \quad (97)$$

for some $\mu_1, \mu_2 > 0$. For more details on this algorithm, we refer the reader to [32].

B - Some Autocorrelation Wavelets and Inner Product Kernels

We present some examples of continuous wavelets along with their corresponding autocovariance wavelets and inner product kernels. Alongside the equations, we also provide visual representations in the form of figures.

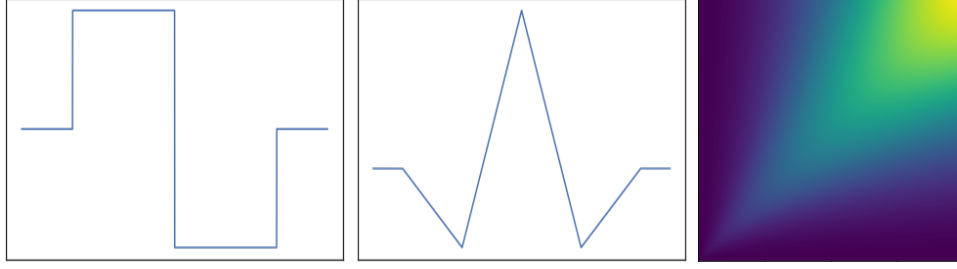


Figure 7: Haar wavelet (left), autocorrelation wavelet (centre) and inner product kernel (right).

Haar Wavelet

The most common and simplest example of a wavelet is the Haar wavelet, which we now discuss. Recall that it has already been defined in a previous section.

Proposition 8. (Autocorrelation Wavelet). Let $u \in \mathbb{R}^+$ and $\tau \in \mathbb{R}$. Then the Haar autocorrelation wavelet is given by

$$\Psi(u, \tau) = \begin{cases} 1 - 3\frac{|\tau|}{u}, & 0 < |\tau| \leq \frac{u}{2}, \\ \frac{|\tau|}{u} - 1, & \frac{u}{2} < |\tau| \leq u, \\ 0, & \text{otherwise.} \end{cases} \quad (98)$$

Proposition 9. (Inner Product Kernel). Let $u, x \in \mathbb{R}^+$. The the Haar inner product kernel is given by

$$A(u, x) = \begin{cases} \frac{x^2}{2u}, & 0 < x \leq \frac{u}{2}, \\ 2x - u + \frac{u^2}{6x} - \frac{5x^2}{6u}, & \frac{u}{2} < x \leq u, \\ 2u - x + \frac{x^2}{6u} - \frac{5u^2}{6x}, & u < x \leq 2u, \\ \frac{u^2}{2x}, & x \geq 2u. \end{cases} \quad (99)$$

Ricker Wavelet

The second wavelet we look at is the Ricker wavelet, which is defined as the negative normalised second derivative of the Gaussian function. In terms of width, it can be considered an intermediate between the Haar and Shannon wavelets. While it does not have compact support, its tails decay rapidly to zero, similar to a Gaussian probability density function.

Definition 27. (Ricker Wavelet). Let $u \in \mathbb{R}^+$ and $x \in \mathbb{R}$. The the Ricker wavelet is defined as

$$\psi(u, x) = \frac{2}{\pi^{1/4}\sqrt{3u}} \left(1 - \frac{x^2}{u^2}\right) e^{-\frac{x^2}{2u^2}}. \quad (100)$$

Proposition 10. (Autocorrelation Wavelet). Let $u \in \mathbb{R}^+$ and $\tau \in \mathbb{R}$. Then the Ricker autocorrelation wavelet is given by

$$\Psi(u, \tau) = \left(1 + \frac{\tau^4}{12u^4} - \frac{\tau^2}{u^2}\right) e^{-\frac{\tau^2}{4u^2}}. \quad (101)$$

Proposition 11. (Inner Product Kernel). Let $u, x \in \mathbb{R}^+$. The the Ricker inner product kernel is given by

$$A(u, x) = \frac{70\sqrt{\pi} u^5 x^5}{3(u^2 + x^2)^{\frac{9}{2}}}. \quad (102)$$

Shannon Wavelet

The final wavelet family we examine is the Shannon wavelet family, which can easily be considered the widest of the three.

Definition 28. (Shannon Wavelet). Let $u \in \mathbb{R}^+$ and $x \in \mathbb{R}$. The the Shannon wavelet is defined as

$$\psi(u, x) = \sqrt{u} \frac{\sin\left(\frac{2\pi x}{u}\right) - \sin\left(\frac{\pi x}{u}\right)}{\pi x}. \quad (103)$$

Its Fourier transform is given by

$$\hat{\psi}(u, \omega) = \sqrt{u} \left(\mathbb{1}_{\left[-\frac{2\pi}{u}, -\frac{\pi}{u}\right]}(\omega) + \mathbb{1}_{\left[\frac{\pi}{u}, \frac{2\pi}{u}\right]}(\omega) \right). \quad (104)$$

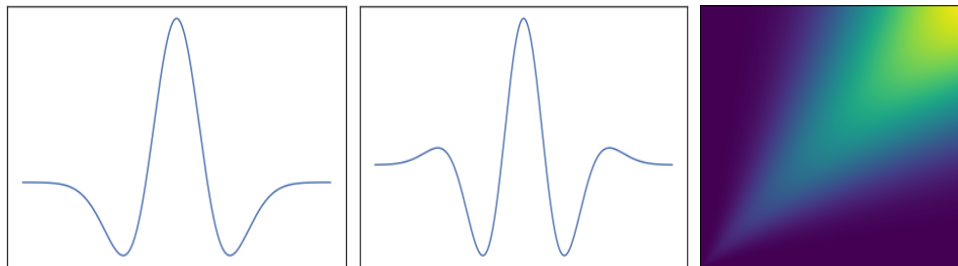


Figure 8: Ricker wavelet (left), autocorrelation wavelet (centre) and inner product kernel (right).

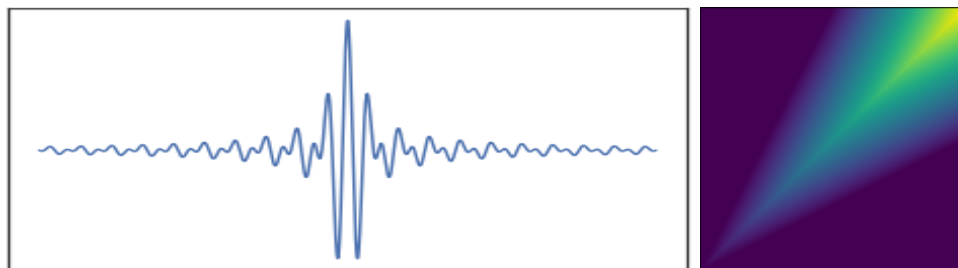


Figure 9: Shannon wavelet and autocorrelation wavelet (left - one is simply a rescaled version of the other) and inner product kernel (right).

Proposition 12. (Autocorrelation Wavelet). Let $u \in \mathbb{R}^+$ and $\tau \in \mathbb{R}$. Then the Shannon autocorrelation wavelet is given by

$$\Psi(u, \tau) = \sqrt{u} \psi(u, \tau). \quad (105)$$

Proposition 13. (Inner Product Kernel). Let $u, x \in \mathbb{R}^+$. The the Shannon inner product kernel is given by

$$A(u, x) = \begin{cases} 2x - u, & \frac{u}{2} \leq x \leq u, \\ 2u - x, & u < x \leq 2u, \\ 0, & \text{otherwise.} \end{cases} \quad (106)$$

C - A Comparison of the Local and Standard Autocovariance Functions

Recall that, for $t, \tau \in \mathbb{R}$, the local autocovariance and the standard autocovariance functions are given by

$$c(t, \tau) = \int_0^\infty S(u, t) \Psi(u, \tau) du \quad (107)$$

and

$$c_X(t, \tau) = \int_0^\infty \int_{-\infty}^\infty S(u, t+v) \psi(u, v) \psi(u, v-\tau) dv du, \quad (108)$$

respectively, as defined in Section 3. In this section we study the difference between the two representations in more detail, using a simple toy example.

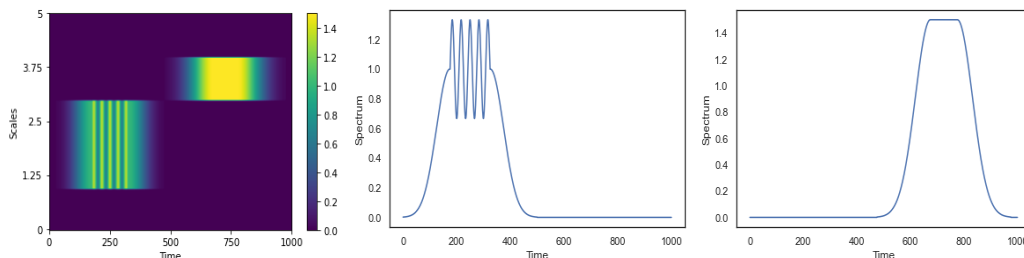


Figure 10: From left to right: the full evolutionary wavelet spectrum and the evolutionary wavelet spectrum at scales $u = 1.5$ and $u = 3.5$.

For scale $u \in \mathbb{R}^+$ and time $t \in \mathbb{R}$, let's consider the evolutionary wavelet spectrum defined as

$$S(u, t) = \begin{cases} \exp\left\{-\left(\frac{x-175}{75}\right)^2\right\}, & \text{for } 1 \leq u \leq 3 \text{ and } 25 \leq t \leq 175, \\ 1 + \frac{1}{3} \sin\left(3 \frac{x-175}{50} \pi\right), & \text{for } 1 \leq u \leq 3 \text{ and } 175 < t \leq 325 \\ \exp\left\{-\left(\frac{x-325}{75}\right)^2\right\}, & \text{for } 1 \leq u \leq 3 \text{ and } 325 < t \leq 475, \\ \frac{3}{2} \exp\left\{-\left(\frac{x-675}{100}\right)^2\right\}, & \text{for } 3 < u \leq 4 \text{ and } 475 < t \leq 675, \\ \frac{3}{2}, & \text{for } 3 < u \leq 4 \text{ and } 675 < t \leq 775, \\ \frac{3}{2} \exp\left\{-\left(\frac{x-775}{100}\right)^2\right\}, & \text{for } 3 < u \leq 4 \text{ and } 775 < t \leq 975 \\ 0, & \text{otherwise.} \end{cases} \quad (109)$$

The evolutionary wavelet spectrum defined above is shown in Figure 10. We have also included plots of the spectrum for scales $u = 1.5$ and $u = 3.5$ in order to more effectively visualise its structure. As can be seen, the spectrum displays a varying degree of behaviours. We re-define the same spectrum for the same scales, but multiplied by factors of 4 and 10 (for example, if the original spectrum is defined for $3 < u < 4$, then the new ones would be defined for $12 < u < 16$ and $30 < u < 40$ respectively). These allow us to compare the two quantities over a larger range of scales.

In the following we take the underlying wavelets to be Ricker wavelets. Although in theory $\psi(u, x) > 0$ for all $x \in \mathbb{R}$ and scales $u \in \mathbb{R}^+$, the tails decay rapidly enough that $\psi(u, x)$ can be considered equal to zero for $x \notin (-4u, 4u)$. Hence the approximate support of these wavelets is $(-4u, 4u)$, making them quite wide functions.

As discussed previously, the local autocovariance at time $t \in \mathbb{R}$ is computed by assuming that the spectrum takes the constant value $S(u, t)$, which due to the fact that the wavelets are non-zero only in a small region around t , this is the same as assuming that the spectrum is constant at a local level rather than a global one. Figure 11 gives further insight into this. On the left we see a plot of several Ricker wavelets; only the region over which they overlap contributes to the autocovariance of the process, this being maximal at $\tau = 0$ (in which case it is equal to the width of the wavelet, $8u$). On the right, we show part of the spectrum. On this, we have also drawn horizontal lines representing the width of the region for which the spectrum is assumed to be constant when computing the local autocovariance. We do this for a range of different scales. Some of the wider ones cover almost the whole range of the spectrum, which is unrealistic in practice, as the spectrum would vary at a significantly slower rate as these coarser scales (see the model interpretation in Section 3 for a more detailed discussion). However, even in this case we will see that the two quantities are very similar. From this visual cue, it is clear that the local autocovariance preserves the structure of the standard autocovariance function, although the values may differ slightly.

We compute the local autocovariance and standard autocovariance functions for the spectrums defined above and the results are displayed in Figure 12. As can be seen, the local autocovariance and standard autocovariance functions are almost indistinguishable, with the ones computed from the spectrum defined at the coarsest scales displaying the most differences, as expected. Therefore, even on a spectrum that varies rapidly, the local and standard autocovariance are very similar. In practice, the spectrum will vary at a slower rate, especially for the coarser scales, and therefore the difference between the two should be even more unnoticeable.

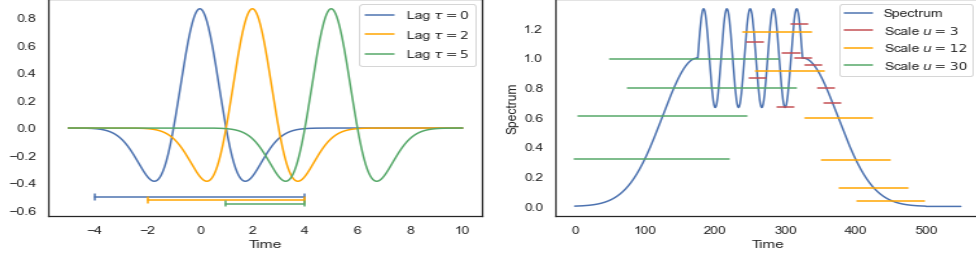


Figure 11: Left: the Ricker wavelet for scale $u = 1$, with shifts corresponding to different values of the lag τ . The horizontal line below denotes the region of overlap, which is the only non-zero contribution to the integral in (107) and (108). Right: the local autocovariance approximates the spectrum with a constant in an interval of length at most equal to the width of the underlying wavelets. The horizontal lines display this for different scales u and times t .

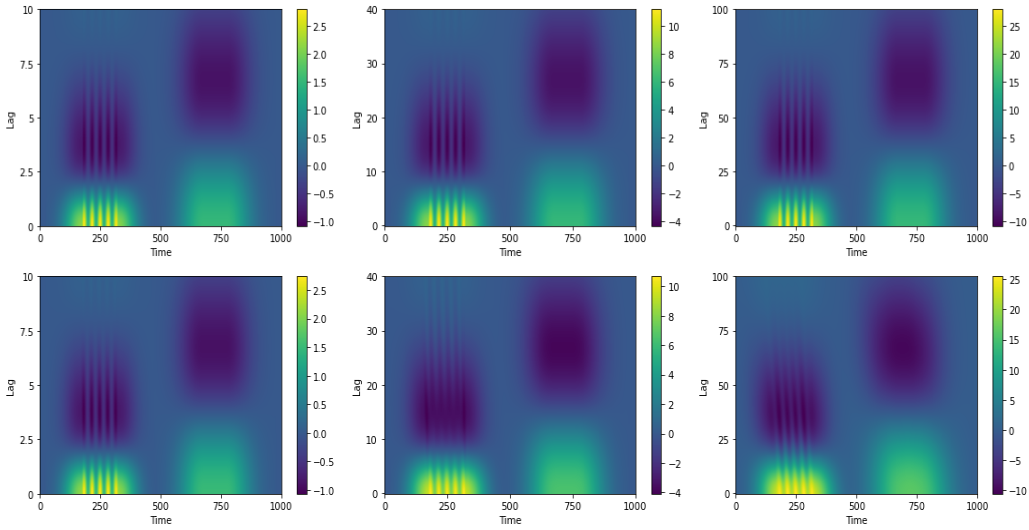


Figure 12: The local autocovariance (top row) and the standard autocovariance (bottom row), computed from the spectrum in (109) defined for scales $0 < u \leq 5$, $0 < u \leq 20$ and $0 < u \leq 100$ (from left to right).

The comparison carried out in this short section carries over quite naturally when examining the difference between the expectation of the raw wavelet periodogram and its approximation, a bound for which was established in Theorem 8. In fact, we expect to obtain similar results, as the spectrum is approximated in the same manner with a larger number of wavelet terms present in the integral. The analysis carried out here only applies to the continuous time version of the model defined in Section 3. When we re-define the model in Section 4, we re-introduce a sequence of stochastic processes, and the difference between the two quantities approaches 0 as we send $T \rightarrow \infty$, due to the re-scaling of time.

D - Non-Stationary Haar Moving Average Spectrum

The functional form of the underlying evolutionary wavelet spectrum used in section 4.3 is given by

$$S(u, z) = \begin{cases} \exp \left\{ - \left[60 \left(z - \frac{1}{30} \right) \right]^2 \right\}, & z \in \left(0, \frac{1}{30} \right) \quad \text{and} \quad u \in (0.5, 1.5) \\ 1, & z \in \left(\frac{1}{30}, \frac{3}{10} \right) \quad \text{and} \quad u \in (0.5, 1.5) \\ \exp \left\{ - \left[60 \left(z - \frac{3}{10} \right) \right]^2 \right\}, & z \in \left(\frac{3}{10}, \frac{1}{3} \right) \quad \text{and} \quad u \in (0.5, 1.5) \\ \exp \left\{ - \left[60 \left(z - \frac{11}{30} \right) \right]^2 \right\}, & z \in \left(\frac{1}{3}, \frac{11}{10} \right) \quad \text{and} \quad u \in (1.5, 2.5) \\ 1, & z \in \left(\frac{11}{30}, \frac{19}{30} \right) \quad \text{and} \quad u \in (1.5, 2.5) \\ \exp \left\{ - \left[60 \left(z - \frac{19}{30} \right) \right]^2 \right\}, & z \in \left(\frac{19}{30}, \frac{2}{3} \right) \quad \text{and} \quad u \in (1.5, 2.5) \\ \exp \left\{ - \left[60 \left(z - \frac{7}{10} \right) \right]^2 \right\}, & z \in \left(\frac{2}{3}, \frac{7}{10} \right) \quad \text{and} \quad u \in (4.5, 5.5) \\ 1, & z \in \left(\frac{7}{10}, \frac{29}{30} \right) \quad \text{and} \quad u \in (4.5, 5.5) \\ \exp \left\{ - \left[60 \left(z - \frac{29}{30} \right) \right]^2 \right\}, & z \in \left(\frac{29}{30}, 1 \right) \quad \text{and} \quad u \in (4.5, 5.5) \end{cases} \quad (110)$$

E - Proofs

Proof of Proposition 1

We have that

$$c_X(t, \tau) = \mathbb{E}[X(t)X(t + \tau)] \quad (111)$$

$$= \int_0^\infty \int_{-\infty}^\infty |W(u, v)|^2 \psi(u, v - t) \psi(u, v - t - \tau) du dv \quad (112)$$

$$= \int_0^\infty \int_{-\infty}^\infty S(u, v + t)^2 \psi(u, v) \psi(u, v - \tau) du dv, \quad (113)$$

where we used that $\mathbb{E}[L(du, dv)L(dx, dy)] = \delta(u - x)\delta(v - y) du dv$ and δ denotes the Dirac delta function. Now, we also have that

$$c(t, \tau) = \int_0^\infty S(u, t) \Psi(u, \tau) du = \int_0^\infty S(u, t) \psi(u, v) \psi(u, v - \tau) du dv, \quad (114)$$

and therefore

$$|c_X(t, \tau) - c(t, \tau)| = \left| \int_0^\infty \int_{-\infty}^\infty (S(u, v + t) - S(u, t)) \psi(u, v) \psi(u, v - \tau) du dv \right| \quad (115)$$

$$\leq \left| \int_0^\infty \int_{-\infty}^\infty |S(u, v + t) - S(u, t)| \psi(u, v) \psi(u, v - \tau) du dv \right| \quad (116)$$

$$= \left| \int_0^\infty \kappa(u) \int_{-\infty}^\infty |v| \psi(u, v) \psi(u, v - \tau) du dv \right| = \theta(\tau), \quad (117)$$

as required. \square

Proof of Proposition 2

(a) Follows from the definition.

(b) $\Psi(u, 0) = \|\psi\|^2 = 1$.

(c) We have that

$$\Psi(u, \tau) = \int_{-\infty}^{\infty} \psi(u, v) \psi(u, v - \tau) dv = \frac{1}{u} \int_{-\infty}^{\infty} \psi\left(\frac{v}{u}\right) \psi\left(\frac{v - \tau}{u}\right) dv \quad (118)$$

$$= \int_{-\infty}^{\infty} \psi(y) \psi\left(y - \frac{\tau}{u}\right) dy = \Psi\left(\frac{x}{u}\right), \quad (119)$$

where we made the substitution $v = uy$.

(d) We have that

$$\Psi(\tau) = \int_{-\infty}^{\infty} \psi(v) \psi(v - \tau) dv = (\psi * \psi)(\tau), \quad (120)$$

where $*$ denotes the convolution operator. Hence

$$\hat{\Psi}(\omega) = \mathcal{F}(\Psi)(\omega) = |\hat{\psi}(\omega)|^2. \quad (121)$$

Since, $\Psi(u, \tau) = \Psi\left(\frac{\tau}{u}\right)$, we have

$$\hat{\Psi}(u, \omega) = \mathcal{F}\left(\Psi\left(\frac{\cdot}{u}\right)\right)(\omega) = u \hat{\Psi}(u\omega) = u |\hat{\psi}(u\omega)|^2. \quad (122)$$

(e) We have

$$\int_{-\infty}^{\infty} \Psi(u, \tau) d\tau = \int_{-\infty}^{\infty} \int_{-\infty}^{\infty} \psi(u, v) \psi(u, v - \tau) dv d\tau \quad (123)$$

$$= \int_{-\infty}^{\infty} \psi(u, v) \int_{-\infty}^{\infty} \psi(u, v - \tau) d\tau dv = 0, \quad (124)$$

as the inner integral is zero. \square

Proof of Proposition 3

Continuity follows from the continuity of the autocovariance wavelets. Symmetry is clear from the definition. We now show that A is non-negative definite. Let $c_i, c_j \in \mathbb{R}$ and $x_i, x_j \in \mathbb{R}^+$ for $i, j = 1, \dots, n$. Then

$$\sum_{i=1}^n \sum_{j=1}^n c_i c_j A(x_i, x_j) = \int_{-\infty}^{\infty} \sum_{i=1}^n \sum_{j=1}^n c_i c_j \Psi(x_i, y) \Psi(x_j, y) dy \quad (125)$$

$$= \int_{-\infty}^{\infty} \left(\sum_{i=1}^n c_i \Psi(x_i, y) \right)^2 dy \geq 0. \quad (126)$$

For the final property, we have

$$A(bx, by) = \int_{-\infty}^{\infty} \Psi(bx, \tau) \Psi(by, \tau) d\tau \quad (127)$$

$$= \int_{-\infty}^{\infty} \Psi\left(\frac{\tau}{bx}\right) \Psi\left(\frac{\tau}{by}\right) d\tau \quad (128)$$

$$= \int_{-\infty}^{\infty} \Psi\left(x, \frac{\tau}{b}\right) \Psi\left(y, \frac{\tau}{b}\right) d\tau \quad (129)$$

$$= b \int_{-\infty}^{\infty} \Psi(x, t) \Psi(y, t) dt \quad (130)$$

$$= bA(x, y), \quad (131)$$

where we used (c) from Proposition 2. \square

Proof of Theorem 1

We have that

$$\beta(u, v) = \mathbb{E}[I(u, v)] = \mathbb{E}\left[\left(\int_{-\infty}^{\infty} X_N(t)\psi(u, t-v)dt\right)^2\right] \quad (132)$$

$$= \int_{-\infty}^{\infty} \int_{-\infty}^{\infty} \mathbb{E}[X_N(t)X_N(s)]\psi(u, t-v)\psi(u, s-v) dt ds \quad (133)$$

Now,

$$\mathbb{E}[X_N(t)X_N(s)] = \int_0^{\infty} \int_{-\infty}^{\infty} |W(x, y)|^2 \psi(x, t-y)\psi(x, s-y) dx dy, \quad (134)$$

where we used the fact that $\mathbb{E}[L(du, dv)L(d\eta, d\gamma)] = \delta(\eta - u)\delta(\gamma - v) du dv$ and again we denoted the Dirac delta function by δ . Hence,

$$\begin{aligned} \beta(u, v) &= \int_{-\infty}^{\infty} \int_{-\infty}^{\infty} \int_0^{\infty} \int_{-\infty}^{\infty} S(x, y)\psi(x, t-y)\psi(x, s-y) dx dy \\ &\quad \psi(u, t-v)\psi(u, s-v) dt ds \end{aligned} \quad (135)$$

$$\begin{aligned} &= \int_{-\infty}^{\infty} \int_{-\infty}^{\infty} \int_0^{\infty} \int_{-\infty}^{\infty} S(x, y+v)\psi(x, t-y-v)\psi(x, s-y-v) \\ &\quad \psi(u, t-v)\psi(u, s-v) dx dy dt ds \end{aligned} \quad (136)$$

$$= \int_{-\infty}^{\infty} \int_{-\infty}^{\infty} \int_0^{\infty} \int_{-\infty}^{\infty} S(x, y+v)\psi(x, t-y)\psi(x, s-y)\psi(u, t)\psi(u, s) dx dy dt ds. \quad (137)$$

Furthermore,

$$\int_0^{\infty} S(x, v) A(u, x) dx = \int_0^{\infty} S(x, v) \int_{-\infty}^{\infty} \Psi(x, \eta)\Psi(u, \eta) d\eta dx \quad (138)$$

$$= \int_0^{\infty} S(x, v) \int_{-\infty}^{\infty} \Psi(x, \eta) \int_{-\infty}^{\infty} \psi(u, \gamma)\psi(u, \gamma + \eta) d\gamma d\eta dx \quad (139)$$

$$= \int_0^{\infty} S(x, v) \int_{-\infty}^{\infty} \int_{-\infty}^{\infty} \Psi(x, \eta)\psi(u, \eta + \gamma)\psi(u, \gamma) d\eta d\gamma dx \quad (140)$$

$$= \int_0^{\infty} S(x, v) \int_{-\infty}^{\infty} \int_{-\infty}^{\infty} \Psi(x, t-s)\psi(u, t)\psi(u, s) dt ds dx, \quad (141)$$

and since

$$\Psi(x, t-s) = \int_{-\infty}^{\infty} \psi(x, r)\psi(x, r - (t-s)) dr = \int_{-\infty}^{\infty} \psi(x, t-y)\psi(x, s-y) dy, \quad (142)$$

we have

$$\begin{aligned} \int_0^{\infty} S(x, v) A(u, x) dx &= \int_{-\infty}^{\infty} \int_{-\infty}^{\infty} \int_0^{\infty} \int_{-\infty}^{\infty} S(x, v)\psi(x, t-y) \\ &\quad \psi(x, s-y)\psi(u, t)\psi(u, s) dx dy dt ds. \end{aligned} \quad (143)$$

Therefore, using the fact that

$$|S(x, y+v) - S(x, v)| \leq \kappa(x) |y|, \quad (144)$$

we have

$$\left| \beta(u, v) - \int_0^{\infty} S(x, v) A(u, x) dx \right| \leq \Omega(u), \quad (145)$$

as required. \square

Proof of Proposition 4

First of all, we have that

$$A(x, x) = \int_{-\infty}^{\infty} \Psi(x, \tau)^2 d\tau > 0. \quad (146)$$

Since A is continuous, we have that for each $x \in \mathbb{R}$, $A(x, y) > 0$ for all $y \in (x - g(x), x + g(x))$, for some function $g(x) > 0$. Now, assume that there exists $f \in N(T_A)$ such that $f \neq 0$. This means that

$$(T_A f)(x) = \int_0^{\infty} A(x, y) f(y) dy = 0, \quad \forall x \in \mathbb{R}^+. \quad (147)$$

Using the fact that $A(\beta x, \beta y) = \beta A(x, y)$ for all $\beta > 0$, we have

$$\int_0^{\infty} A(x, y) f(y) dy = \int_0^{\infty} x A\left(1, \frac{y}{x}\right) f(y) dy = \int_0^{\infty} x^2 A(1, u) f(xu) du, \quad (148)$$

where we used the substitution $y = xu$. Hence (147) becomes

$$\int_0^{\infty} A(1, u) f(xu) du = 0, \quad \forall x \in \mathbb{R}^+, \quad (149)$$

or equivalently

$$\langle A(1, \cdot), f(x \cdot) \rangle = 0 \quad \forall x \in \mathbb{R}^+, \quad (150)$$

which implies that $A(1, u) = 0$ for all $u \in \mathbb{R}^+$, a contradiction. Hence $N(T_A) = \{0\}$. \square

Proof of Theorem 2

Multiplying both sides of

$$c(t, \tau) = \int_0^{\infty} S(u, t) \Psi(u, \tau) du, \quad (151)$$

by $\Psi(u, \tau)$ and integrating, we have

$$\int_{-\infty}^{\infty} c(z, \tau) \Psi(u, \tau) d\tau = \int_0^{\infty} S(x, z) A(u, x) dx = (T_A S(\cdot, z))(u), \quad (152)$$

which, using the inverse of

$$(T_A f)(x) = \sum_{n=1}^{\infty} \lambda_n \langle \varphi_n, f \rangle \varphi_n(x), \quad (153)$$

we obtain

$$S(u, z) = \frac{1}{\sqrt{\alpha}} \sum_{n=1}^{\infty} \frac{1}{\lambda_n} \varphi_n(u) \int_{-\infty}^{\infty} c(z, \tau) \langle \Psi(\cdot, \tau), \varphi_n \rangle d\tau, \quad (154)$$

as required. \square

Proof of Proposition 5

We have that

$$c_{X_T}(t, \tau) = \mathbb{E}[X_T(t) X_T(t + \tau)] \quad (155)$$

$$= \int_0^{J_\psi(T)} \int_{-\infty}^{\infty} |w_T(u, v)|^2 \psi(u, v - t) \psi(u, v - t - \tau) du dv \quad (156)$$

$$= \int_0^{J_\psi(T)} \int_{-\infty}^{\infty} |w_T(u, v + t)|^2 \psi(u, v) \psi(u, v - \tau) du dv, \quad (157)$$

where we used that $\mathbb{E}[L(du, dv) L(dx, dy)] = \delta_{u,x} \delta_{v,y} du dv$. Now, from condition (c) in Definition 10, we have that

$$\left| w_T(u, v + t) - W\left(u, \frac{v + t}{T}\right) \right| \leq \frac{C(u)}{T}. \quad (158)$$

Furthermore, from the Lipschitz continuity of W , we also have that

$$\left| S\left(u, \frac{v+t}{T}\right) - S\left(u, \frac{t}{T}\right) \right| \leq \kappa(u) \left| \frac{v}{T} \right| \quad (159)$$

from which it follows that

$$\left| |w_T(u, v+t)|^2 - S\left(u, \frac{t}{T}\right) \right| \leq \frac{1}{T} (C(u) + |v| \kappa(u)) \quad (160)$$

Therefore,

$$|c_{X_T}(t, \tau) - c(z, \tau)| = \left| \int_0^{J_\psi(T)} \int_{-\infty}^{\infty} (|w_T(u, v+t)|^2 - S\left(u, \frac{t}{T}\right)) \psi(u, v) \psi(u, v-\tau) du dv \right| \quad (161)$$

$$\leq \int_0^{J_\psi(T)} \int_{-\infty}^{\infty} \left| |w_T(u, v+t)|^2 - S\left(u, \frac{t}{T}\right) \right| |\psi(u, v) \psi(u, v-\tau)| du dv \quad (162)$$

$$\leq \frac{1}{T} \left| \int_0^{J_\psi(T)} \int_{-\infty}^{\infty} (C(u) + |v| \kappa(u)) \psi(u, v) \psi(u, v-\tau) du dv \right| \quad (163)$$

$$= O(T^{-1}), \quad (164)$$

since the integrals are finite, as required. \square

Proof of Theorem 3

Some steps are quite similar to the proof of Proposition 1 and Theorem 4, and so in the following we skip some details. We have that

$$\beta(u, z) = \beta\left(u, \frac{v}{T}\right) = \mathbb{E} [|d(u, v)|^2] = \mathbb{E} \left[\left(\int_{-\infty}^{\infty} X_T(t) \psi(u, t-v) dt \right)^2 \right] \quad (165)$$

$$= \int_{-\infty}^{\infty} \int_{-\infty}^{\infty} \mathbb{E}[X_T(t) X_T(s)] \psi(u, t-v) \psi(u, s-v) dt ds \quad (166)$$

Now,

$$\mathbb{E}[X_T(t) X_T(s)] = \int_0^{J_\psi(T)} \int_{-\infty}^{\infty} |w_T(x, y)|^2 \psi(x, t-y) \psi(x, s-y) dx dy, \quad (167)$$

where we used that $\mathbb{E}[L(du, dv)L(d\eta, d\gamma)] = \delta_{\eta, x} \delta_{\gamma, y} du dv$. Hence,

$$\beta(u, z) = \int_0^{J_\psi(T)} \int_{-\infty}^{\infty} |w_T(x, y)|^2 \int_{-\infty}^{\infty} \int_{-\infty}^{\infty} \psi(x, t-y) \psi(x, s-y) \psi(u, t-v) \psi(u, s-v) dt ds dy dx \quad (168)$$

$$= \int_0^{J_\psi(T)} \int_{-\infty}^{\infty} |w_T(x, y+v)|^2 \int_{-\infty}^{\infty} \int_{-\infty}^{\infty} \psi(x, t-y-v) \psi(x, s-y-v) \psi(u, t-v) \psi(u, s-v) dt ds dy dx \quad (169)$$

$$= \int_0^{J_\psi(T)} \int_{-\infty}^{\infty} |w_T(x, y+v)|^2 \int_{-\infty}^{\infty} \int_{-\infty}^{\infty} \psi(x, t-y) \psi(x, s-y) \psi(u, t) \psi(u, s) dt ds dy dx. \quad (170)$$

Using similar steps as in the proof of Theorem 4,

$$\int_0^{J_\psi(T)} S(x, z) A(u, x) dx = \int_0^{J_\psi(T)} \int_{-\infty}^{\infty} S\left(x, \frac{v}{T}\right) \int_{-\infty}^{\infty} \int_{-\infty}^{\infty} \psi(x, t-y) \psi(x, s-y) \psi(u, t) \psi(u, s) dt ds dy dx \quad (171)$$

and using the fact that

$$\left| |w_T(u, v + t)|^2 - S\left(u, \frac{t}{T}\right) \right| \leq \frac{1}{T}(C(u) + |v| \kappa(u)), \quad (172)$$

we have

$$\left| \beta(u, z) - \int_0^{J_\psi(T)} S(x, z) A(u, x) dx \right| \leq O(T^{-1}), \quad (173)$$

as required. \square

Proof of Proposition 8

We have that

$$\Psi(\tau) = \int_{-\infty}^{\infty} \psi(x) \psi(x - \tau) dx \quad (174)$$

$$= \int_{-\infty}^{\infty} \left(\mathbb{1}_{[0, \frac{1}{2}]}(x) - \mathbb{1}_{[\frac{1}{2}, 1]}(x) \right) \left(\mathbb{1}_{[0, \frac{1}{2}]}(x - \tau) - \mathbb{1}_{[\frac{1}{2}, 1]}(x - \tau) \right) dx \quad (175)$$

$$= \int_{-\infty}^{\infty} \left(\mathbb{1}_{[0, \frac{1}{2}]}(x) - \mathbb{1}_{[\frac{1}{2}, 1]}(x) \right) \left(\mathbb{1}_{[\tau, \frac{1}{2} + \tau]}(x) - \mathbb{1}_{[\frac{1}{2} + \tau, 1 + \tau]}(x) \right) dx \quad (176)$$

$$= \int_{-\infty}^{\infty} \mathbb{1}_{[0, \frac{1}{2}] \cap [\tau, \frac{1}{2} + \tau]}(x) - \mathbb{1}_{[\frac{1}{2}, 1] \cap [\tau, \frac{1}{2} + \tau]}(x) \\ - \mathbb{1}_{[0, \frac{1}{2}] \cap [\frac{1}{2} + \tau, 1 + \tau]}(x) + \mathbb{1}_{[\frac{1}{2}, 1] \cap [\frac{1}{2} + \tau, 1 + \tau]}(x) dx \quad (177)$$

$$= 2 \left(\frac{1}{2} - |\tau| \right) \mathbb{1}_{[-\frac{1}{2}, \frac{1}{2}]}(\tau) - \left(\frac{1}{2} - \left| \tau - \frac{1}{2} \right| \right) \mathbb{1}_{[0, 1]}(\tau) \\ - \left(\frac{1}{2} - \left| \tau + \frac{1}{2} \right| \right) \mathbb{1}_{[-1, 0]}(\tau) \quad (178)$$

$$= \begin{cases} 1 - 3|\tau|, & 0 < |\tau| \leq \frac{1}{2}, \\ |\tau| - 1, & \frac{1}{2} < |\tau| \leq 1, \\ 0, & \text{otherwise.} \end{cases} \quad (179)$$

Then, using property (iii) from Proposition 6,

$$\Psi(u, \tau) = \begin{cases} 1 - 3\frac{|\tau|}{u}, & 0 < |\tau| \leq \frac{u}{2}, \\ \frac{|\tau|}{u} - 1, & \frac{u}{2} < |\tau| \leq u, \\ 0, & \text{otherwise,} \end{cases} \quad (180)$$

as required. \square

Proof of Proposition 9

We have

$$A(u, x) = \int_{-\infty}^{\infty} \Psi(u, y) \Psi(x, y) dy \quad (181)$$

$$= \int_{-\infty}^{\infty} \left(\left(1 - 3\frac{|y|}{u} \right) \mathbb{1}_{[0, \frac{u}{2}]}(|y|) + \left(\frac{|y|}{u} - 1 \right) \mathbb{1}_{[\frac{u}{2}, u]}(|y|) \right) \\ \left(\left(1 - 3\frac{|y|}{x} \right) \mathbb{1}_{[0, \frac{x}{2}]}(|y|) + \left(\frac{|y|}{x} - 1 \right) \mathbb{1}_{[\frac{x}{2}, x]}(|y|) \right) dy \quad (182)$$

By evaluating each of the terms in the above individually, the required result is obtained in a straightforward manner. \square

Proof of Proposition 10

We have that

$$\Psi(u, \tau) = \int_{-\infty}^{\infty} \psi(u, x)\psi(u, x - \tau) dx \quad (183)$$

$$= \frac{4}{3u\sqrt{\pi}} \int_{-\infty}^{\infty} \left(1 - \frac{x^2}{u^2}\right) \left(1 - \frac{(x - \tau)^2}{u^2}\right) \exp\left\{-\frac{x^2 + (x - \tau)^2}{2u^2}\right\} dx \quad (184)$$

$$= \frac{4}{3u\sqrt{\pi}} \int_{-\infty}^{\infty} \left(1 - \frac{x^2 + (x - \tau)^2}{u^2} + \frac{x^2(x - \tau)^2}{u^4}\right) \exp\left\{-\frac{(x - \frac{\tau}{2})^2 + \frac{\tau^2}{4}}{u^2}\right\} dx \quad (185)$$

$$= \frac{4e^{-\frac{\tau^2}{4u^2}}}{3u\sqrt{\pi}} \int_{-\infty}^{\infty} \left(1 - 2\frac{(x - \frac{\tau}{2})^2 + \frac{\tau^2}{4}}{u^2} + \frac{x^2(x - \tau)^2}{u^4}\right) \exp\left\{-\frac{(x - \frac{\tau}{2})^2}{u^2}\right\} dx, \quad (186)$$

where we completed the square in the exponential. Now, setting

$$y = \sqrt{2} \frac{x - \frac{\tau}{2}}{u}, \quad (187)$$

we have

$$\Psi(u, \tau) = \frac{4}{3} e^{-\frac{\tau^2}{4u^2}} \int_{-\infty}^{\infty} \left(1 - \frac{\tau^2}{2u^2} + \frac{\tau^4}{16u^4} - \left(1 + \frac{\tau^2}{4u^2}\right) y^2 + \frac{1}{4} y^4\right) \frac{1}{2\sqrt{\pi}} e^{-\frac{y^2}{2}} dy \quad (188)$$

$$= \frac{4}{3} e^{-\frac{\tau^2}{4u^2}} \left(1 - \frac{\tau^2}{2u^2} + \frac{\tau^4}{16u^4} - \left(1 + \frac{\tau^2}{4u^2}\right) + \frac{3}{4}\right) \quad (189)$$

$$= \left(1 + \frac{\tau^4}{12u^4} - \frac{\tau^2}{u^2}\right) e^{-\frac{\tau^2}{4u^2}}, \quad (190)$$

where we used the fact that we are integrating against the probability density function of a standard normal distribution and so can use its moments. \square

Proof of Proposition 11

We have

$$A(u, x) = \int_{-\infty}^{\infty} \Psi(u, y)\Psi(x, y) dy \quad (191)$$

$$= \int_{-\infty}^{\infty} \left(1 + \frac{\tau^4}{12u^4} - \frac{\tau^2}{u^2}\right) \left(1 + \frac{\tau^4}{12x^4} - \frac{\tau^2}{x^2}\right) \exp\left\{-\frac{\tau^2}{4u^2} - \frac{\tau^2}{4x^2}\right\} d\tau \quad (192)$$

$$= \int_{-\infty}^{\infty} \left(1 - \left(\frac{1}{x^2} + \frac{1}{u^2}\right) \tau^2 + \left(\frac{1}{12u^4} + \frac{1}{x^2u^2} + \frac{1}{12x^4}\right) \tau^4 - \frac{1}{12} \left(\frac{1}{u^2x^4} + \frac{1}{u^4x^2}\right) \tau^6 + \frac{1}{144u^4x^4} \tau^8\right) \exp\left\{-\frac{1}{4} \left(\frac{1}{u^4} + \frac{1}{x^4}\right) \tau^2\right\} d\tau. \quad (193)$$

Setting

$$y^2 = \frac{1}{2} \left(\frac{1}{u^2} + \frac{1}{x^2}\right) \tau^2, \quad (194)$$

we have

$$A(u, x) = 2\sqrt{\frac{\pi u^2 x^2}{u^2 + x^2}} \int_{-\infty}^{\infty} \left(1 - 2y^2 + \frac{1}{3}y^4 + \frac{10u^2x^2}{3(u^2 + x^2)^2}y^4 - \frac{2u^2x^2}{3(u^2 + x^2)^2}y^6 + \frac{u^4x^4}{9(u^2 + x^2)^4}y^8\right) \frac{1}{2\pi} e^{-\frac{y^2}{2}} dy \quad (195)$$

$$= 2\sqrt{\frac{\pi u^2 x^2}{u^2 + x^2}} \left(1 - 2 + 1 + \frac{10u^2x^2}{(u^2 + x^2)^2} - \frac{10u^2x^2}{(u^2 + x^2)^2} + \frac{35u^4x^4}{3(u^2 + x^2)^4}\right) \quad (196)$$

$$= \frac{70\sqrt{\pi}}{3} \frac{u^5x^5}{(u^2 + x^2)^{\frac{9}{2}}}, \quad (197)$$

where again we used the fact that we are integrating against the probability density function of a standard normal. \square

Proof of Proposition 12

To begin with, we have that

$$\Psi(u, \tau) = \int_{-\infty}^{\infty} \psi(u, x)\psi(u, x - \tau)dx = \int_{-\infty}^{\infty} \psi(u, x)\psi(u, \tau - x)dx = \psi(u, \cdot) * \psi(u, \cdot) \quad (198)$$

as Shannon wavelets are symmetric and where $*$ denotes the convolution operator. Hence

$$\hat{\Psi}(u, \omega) = \hat{\psi}(u, \omega)\hat{\psi}(u, \omega) = \sqrt{u} \hat{\psi}(u, \omega), \quad (199)$$

since the square of an indicator function is simply equal to the indicator function and the cross term is zero since the intervals are non-overlapping. Hence, taking the inverse Fourier transform

$$\Psi(u, \tau) = \sqrt{u} \psi(u, \tau), \quad (200)$$

as required. \square

Proof of Proposition 13

We have

$$A(u, x) = \int_{-\infty}^{\infty} \Psi(u, y)\Psi(x, y) dy \quad (201)$$

$$= \sqrt{ux} \int_{-\infty}^{\infty} \psi(u, y)\psi(x, y) dy \quad (202)$$

$$= \sqrt{ux} \int_{-\infty}^{\infty} \psi(u, y)\psi(x, -y) dy \quad (203)$$

$$= \sqrt{ux} \mathcal{F}^{-1}(\hat{\psi}(u, \cdot)\hat{\psi}(x, \cdot))(0) \quad (204)$$

where we used the convolution theorem and $\mathcal{F}^{-1}(f)(0)$ denotes the inverse Fourier transform of the function f evaluated at zero. Now, for $x > 2u$, the above is clearly zero as none of the intervals in the indicator functions overlap. For $u \leq x \leq 2u$, we have

$$\hat{\psi}(u, \omega)\hat{\psi}(x, \omega) = \sqrt{ux} \left(\mathbb{1}_{[-\frac{2\pi}{x}, -\frac{\pi}{u}]}(\omega) + \mathbb{1}_{[\frac{\pi}{u}, \frac{2\pi}{x}]}(\omega) \right) \quad (205)$$

The case $x < u$ is symmetrical. Taking the inverse Fourier transform of the above, we obtain

$$\mathcal{F}^{-1}(\hat{\psi}(u, \cdot)\hat{\psi}(x, \cdot))(y) = \frac{\sqrt{ux}}{2\pi} \int_{-\frac{2\pi}{x}}^{-\frac{\pi}{u}} e^{i2\pi\omega y} d\omega + \frac{1}{2\pi} \int_{\frac{\pi}{u}}^{\frac{2\pi}{x}} e^{i2\pi\omega y} d\omega \quad (206)$$

$$= \frac{\sqrt{ux}}{i4\pi^2 y} \left(e^{i4\pi^2 \frac{y}{x}} - e^{i2\pi^2 \frac{y}{u}} + e^{-i2\pi^2 \frac{y}{u}} + e^{-i4\pi^2 \frac{y}{x}} \right) \quad (207)$$

$$= \frac{\sqrt{ux}}{2\pi^2 y} \left(\sin\left(\frac{4\pi^2 y}{x}\right) - \sin\left(\frac{2\pi^2 y}{x}\right) \right) \quad (208)$$

Now,

$$\frac{\sqrt{ux}}{2\pi^2 y} \left(\sin\left(\frac{4\pi^2 y}{x}\right) - \sin\left(\frac{2\pi^2 y}{x}\right) \right) \rightarrow \sqrt{ux} \left(\frac{2}{x} - \frac{1}{u} \right), \quad \text{as } y \rightarrow 0, \quad (209)$$

since

$$\lim_{y \rightarrow 0} \frac{\sin(\alpha y)}{y} = \alpha. \quad (210)$$

Hence, we have $A(u, x) = 2u - x$, $u \leq x \leq 2u$ and the rest follows by symmetry. \square